Journal of Civil Engineering and Construction Technology

Volume 6 Number 3 April 2015

ISSN 2141-2634

Academic Journals

ABOUT JCECT

Journal of Civil Engineering and Construction Technology (ISSN 2141-2634) is published monthly (one volume per year) by Academic Journals.

Journal of Civil Engineering and Construction Technology (JCECT) is an open access journal that provides rapid publication (monthly) of articles in all areas of the subject such as surveying, environmental engineering, hydrology, soil mechanics, shear moments and forces etc. The Journal welcomes the submission of manuscripts that meet the general criteria of significance and scientific excellence. Papers will be published shortly after acceptance. All articles published in JCECT are peer-reviewed.

Contact Us

Editorial Office: jcect@academicjournals.org

Help Desk: helpdesk@academicjournals.org

Website: http://www.academicjournals.org/journal/JCECT

Submit manuscript online http://ms.academicjournals.me/

Editors

Editorial Board

Journal of Civil Engineering and Construction

Table of Contents: Volume 6 Number 2 March 2015

ARTICLES

Research Articles

academicJournals

Vol. 6(3), pp. 15-26, April 2015
DOI:10.5897/JCECT2015.0357
ISSN 2141-2634
Articles Number: CDEA8F552269

http://www.academicjournals.org/JCECT

Journal of Civil Engineering and Construction Technology

Full Length Research Paper

Predicting complex shear modulus using artificial neural networks

Abdulhaq Hadi Abedali

School of Engineering, University of Liverpool, Liverpool, United Kingdom.
Highway and Transportation Department, Engineering College, The University of Mustansiriyah, Baghdad, Iraq.

Received 1 February, 2015; Accepted 30 March, 2015

Developing a predictive model for complex shear modulus of the asphalt binder is a complex technique due to several factors that affect the model's estimating capability, such as rheological properties and test conditions. Several models were developed in this regard; some of these are linear regression models and relate to rheological properties of asphalt binder. A computational model based on artificial neural networks (ANNs) was used for developing models to predict complex shear modulus of the asphalt binder tested in DSR. In this study, two G* prediction models were developed and implemented based on experimental observations: Artificial Neural Network (ANN) model and Multi Linear Regression (MLR) model. A Feed Forward Neural Network (FFNN) model was applied to predict the G*. In order to evaluate the incomes of the two models, statistical parameters were used to make the comparison between them. These parameters include the correlation coefficient (R) and Average Percentage of Error (APE). The data set that has been used in this study includes temperature, frequency, phase angle, dynamic shear viscosity, shear stress and strain. The models were trained with 75% of experimental data. The ANN and MLR approaches were applied to the data to derive the weights and the regression coefficients respectively. The performance of the model was evaluated by using the remaining 25% of the data. By comparing the R^2 of the models, the study reveals that the ANN model can be used as an appropriate forecasting tool to predict the G*, as it out-performs the MLR model.

Key words: Complex shear modulus, artificial neural network analysis, dynamic shear rheometer, multi-linear regression model.

INTRODUCTION

In-situ pavements are under repeated dynamic loading. In this study, a dynamic shear rheometer was used in order to simulate this repeated loading and, in order to obtain the viscoelastic material parameters, sinusoidal shear strains were imposed on asphalt binder samples (Poulikakos and Partl, 2012).

The dynamic shear rheometer (DSR) is used to evaluate rheological properties of asphalt binders fromlow to high temperatures. An understanding of the rheological properties of asphalt binders is essential for predicting the end-use performance of these materials. The DSR measures the complex shear modulus G* and phase

* E-mail: Abdulhaq@liverpool.ac.uk; abdulhaq1969@gmail.com

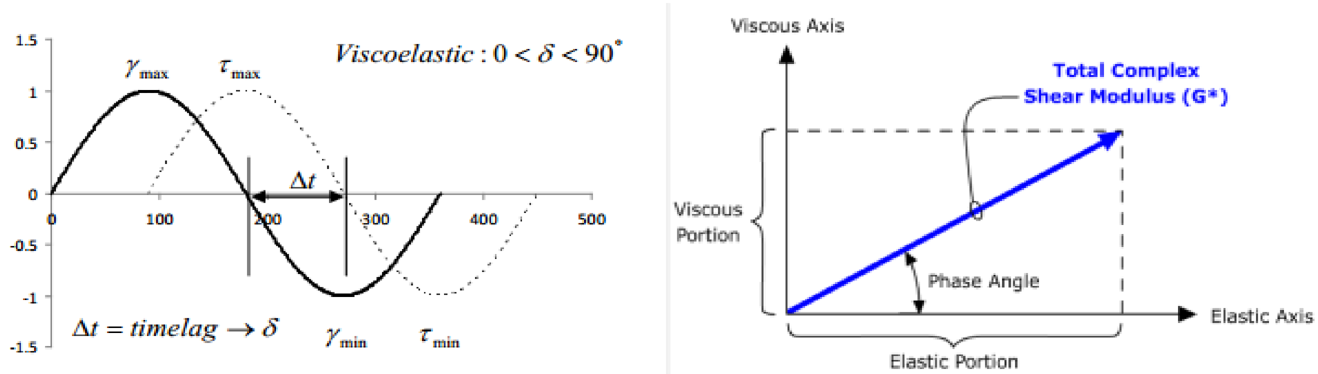

Figure 1. Definition of the phase angle.

angle δ over a wide range of temperatures and frequencies. The complex shear modulus and phase angle are both used in the Superpave specification for the grading of asphalt cements for fatigue and rutting.

Two important parameters are obtained from the dynamic shear rheometer test on asphalt: G*, the complex shear modulus and δ, the phase angle. These parameters can be used to characterise both viscous and elastic behaviour of the material.

When the binder samples are cold, they can behave like an elastic solid where the stress follows the input strain. At elevated temperatures, the material behaves like a Newtonian fluid where the stress lags behind the strain and maximum stress will occur when the rate of strain is the greatest, which is 90° out of phase with the peak strain. In between the two extremes, the material behaviour is viscoelastic and peak stress lags behind peak strain anywhere between 0 and 90°, the phase shift δ, as shown in Figure 1.

The testing is done using shear strains that are small and within the linear viscoelastic region for the material. This allows combining data at lower and higher temperatures and frequencies using the principle of superposition. Dynamic shear rheometer resolves the dynamic elastic and viscous moduli of a binder over a variety of temperatures and loading frequencies.

The sinusoidal alteration of the stress is at a frequency *f* in cycles/s (Hz) or ω (2πf) in radians/s.

Assuming harmonic uniaxial displacement control, we have (Lytton et al., 1993):

$$\varepsilon_t = \varepsilon_0 Sin(\omega t) \; with \; \omega = 2\pi f = 2\pi / t \tag{1}$$

$$\sigma_t = \sigma_0 Sin(\omega t + \delta) \tag{2}$$

With stress and strain amplitude σ_0 and ε_0 respectively and δ is phase angle.

$$G^{/} = \frac{\sigma_0}{\varepsilon_0} * Cos\,(\delta) \tag{3}$$

$$G^{//} = \frac{\sigma_0}{\varepsilon_0} * Sin\,(\delta) \tag{4}$$

$$tan\,(\delta)^{/} = \frac{G^{//}}{G^{/}} \tag{5}$$

The tan (δ) parameter is an important indicator of whether or not an asphalt binder behaves as brittle elastic solid or whether it maintains a viscous component. High values of the tan (δ) indicate that the material maintains its viscous properties – a property that is desirable at low temperatures. Low values of tan (δ) are desirable at high temperatures since they indicate that the elastic properties are maintained and there is better performance under creep loading (Goodrich, 1988). Furthermore, using the definition of a complex shear modulus the $G^{/}$ and $C^{//}$ can be further interpreted.

Similarly, the dynamic viscosity can be calculated as follows:

$$G^* = |G^*|(\cos\delta + i\sin\delta) = |G^*| * e^{i\delta} \tag{6}$$

$$\text{For } |G^*| = \frac{\sigma_0}{\varepsilon_0} \tag{7}$$

$$G^* = \frac{\sigma_0}{\varepsilon_0} cos\,\delta + i\frac{\sigma_0}{\varepsilon_0} sin\delta = G^{/} + iG^{//} \tag{8}$$

$$|G^*| = \sqrt{(G^{/})^2 + (G^{//})^2} \tag{9}$$

The dynamic viscosity can be calculated as follows:

$$\varepsilon_t = \varepsilon_0 * e^{i\omega t} \tag{10}$$

$$\dot{\varepsilon}_t = i\omega\varepsilon_0 * e^{i\omega t} = i\omega\varepsilon_{(t)} \tag{11}$$

The dynamic shear viscosity can be defined as the ratio of stress to strain rate:

$$\eta^* = \frac{\tau}{\dot{\varepsilon}_{(t)}} = \frac{\varepsilon_{(t)} * G^*}{i\omega\,\varepsilon_{(t)}} = \frac{G^*}{i\omega} \tag{12}$$

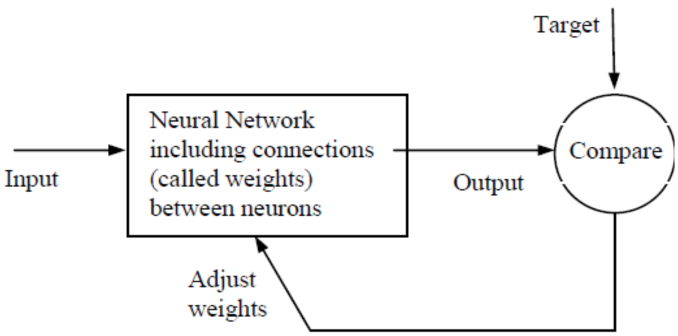

Figure 2. Basic principle of artificial neural networks (Priddy and Keller, 2005).

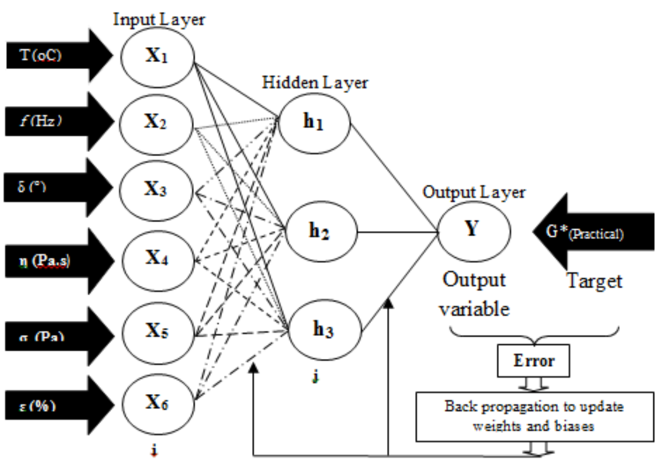

Figure 3. Typical three layers of Feed-Forward ANN.

$$\eta^{/} = \frac{G^{//}}{\omega} \tag{13}$$

$$\eta^{//} = \frac{G^{/}}{\omega} \tag{14}$$

$$|\eta^{*}| = \sqrt{(\eta^{/})^2 + (\eta^{//})^2} = \frac{\sqrt{(G^{/})^2 + (G^{//})^2}}{\omega} \tag{15}$$

Where: ε=strain (%), σ = stress (Pa),
G*=complex shear modulus (Pa), with $G^{/}$ and $G^{//}$ the real and imaginary part of the complex shear modulus respectively.

η*=complex shear viscosity (Pa s), with $\eta^{/}$ and $\eta^{//}$ the real and imaginary part of the complex shear viscosity respectively.

With minimal viscoelastic behaviour, that is pure elastic behaviour, as δ approaches zero, it follows from the above that the storage modulus $G^{/}$=1 and the loss modulus $G^{//}$=0. As δ approaches 90°, that is maximum phase shift and pure viscous response, then $G^{/}$=0 and $G^{//}$=1.

ARTIFICIAL NEURON NETWORK MODEL (ANN)

Neural networks are composed of simple elements operating in parallel. These elements are inspired by biological neurons systems. As in nature, the network function is determined largely by the connections between elements. A neural network can be trained to perform a particular function by adjusting the values of the connections (weights) between the elements. Commonly, neural networks are adjusted, or trained, so that a particular input leads to a specific target output. Such a situation is shown in Figure 2. Here, the network is adjusted based on a comparison of the output and the target, until the sum of square differences between the target and output values becomes the minimum.

Typically, many such input/target output pairs are used to train a network. Batch training of a network proceeds by making weight and bias changes based on an entire set (batch) of input vectors. Incremental training changes the weights and biases of a network as needed after presentation of each individual input vector.

Feed forward ANNs are comprised of a system of neurons, which are arranged in layers. Between the input and output layers, there may be one or more hidden layers. The neurons in each layer are connected to the neurons in a subsequent layer by a weight, *w*, which may be adjusted during training. A data pattern comprising the values *Xi* present at the input layer *i* is propagated forward through the network towards the first hidden layer, *j*. Each hidden neuron receives the weighted outputs *WijXij* from the neurons in the previous layer. These are summed to produce a net value, which is then transformed to an output value upon the application of an activation function (Priddy and Keller, 2005). A typical three-layer feed-forward ANN is shown in Figure 2.

In Figure 3, a typical ANN, which is used in this study, consists of three layers, namely input, hidden and output layers. Input layer neurons are X_o, X_1, X_5; hidden layer neurons are h_1, h_2 and h_3; and output layer neurons are Y_1.

A neuron consists of multiple inputs and a single output. The sum of the inputs and their weights leads to a summation operation as:

$$NET_j = \sum_{i=1}^{n=5} W_{ij} X_{ij} + \theta \tag{16}$$

In which W_{ij} is established weight, X_{ij} is input value, θ is bias that additional inputs with unitary connection weighs and NET_j is input to a node in layer *j*.

The output of a neuron is decided by an activation function. There are a number of activation functions that can be used in ANNs such as step, sigmoid, threshold, linear, etc. The sigmoid activation function, $f_{(x)}$, commonly used and applied in this study, can be formulated mathematically as:

$$f_{(x)} = \frac{1}{1+e^{-x}} \tag{17}$$

$$Output_j = f(NET_j) = \frac{1}{1+e^{-NET_j}} \tag{18}$$

Research objectives

The following objectives were assigned for this study:

1) Predicting the complex shear modulus of asphalt binder tested in DSR and evaluated according to six parameters (test temperature,

Table 1. Properties of the asphalt binder.

Property	Nasiriyah	Durah
Penetration (0.1 mm, 100 g and 5 s)- ASTM D5	41	43
Softening point (°C) - ASTM D36	52	53
Penetration Index (PI)	-1.0	-0.35
Viscosity cP, 135 (°C) -ASTM D 4402	500	481.3

Table 2. Summary of the properties of elastomer used (Kraton Polymers, 2006).

Property	D 1101 K SBS	D 1184 K SBS
Tensile strength (PSI).	4,600	4,000
Elongation (%)	880	820
Specific gravity	0.94	0.94
Brookfield viscosity (cps at 77°F)	4,000	20,000
Diblock (%)	16	16
300% modulus (PSI)	400	800
Molecular structure	Linear	Radial

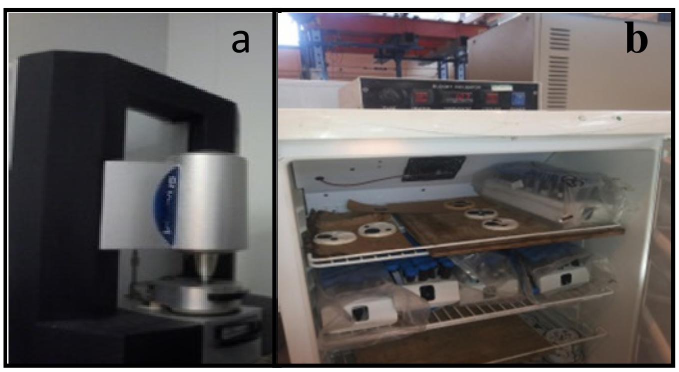

Figure 4. a) Kinexus Pro^{+} DSR b) Silicon moulds in fridge.

applied frequency, phase angle, dynamic shear viscosity, applied shear stress and strain).These parameters were nominated as independent variables for developing regression and ANN models.
2) Using the ANN process for predicting complex shear modulus of modified asphalt binders tested in DSR using the results, which were obtained from pure asphalt binder.

EXPERIMENTAL DESIGN

Materials

The conventional bitumen samples were acquired from two sources (Nasiriyah and Durah Refineries) in the middle and southern regions of Iraq, where they are commonly used; they have (40 to 50) penetration grade. Two types of styrene-butadiene-styrene (SBS) at three different modification levels, namely 3, 6 and 9%, by weight of the bitumen are used to modify the rheological properties of asphalt binder. The properties of asphalt binders are shown in Tables 1 and 2.

Sample preparation and test conditions

The asphalt binder was preheated in an oven to the recommended temperature (160±5°C) for the unmodified binders and (160±5°C) for the modified binders. Samples should be stirred before being poured into a silicon mould as the received sample must be homogenised when it is poured in. The silicon moulds are then used to prepare samples for frequency sweep, as seen in Figure 4b. Frequency sweep tests were conducted with an 8 mm diameter plate with a 2 mm testing gap and a 25 mm diameter plate with a 1 mm testing gap. The selection of the testing geometry is based on the operational conditions, with the 8 mm plate geometry generally being used at low temperatures (5 to 25°C) and the 25 mm geometry at intermediate to high temperatures (35 to 60°C) (BS EN 14770, 2012).

The sample is loaded into the rheometer within 60 min of moulding. The temperature of the rheometer plates during loading should be high enough in order to assure good adhesion to the plates. In the case of unmodified binders, a 60°C temperature is recommended. In any case, the sample should start flowing to get good adhesion to both plates (the gap is first decreased to 2.05 mm). The sample is cooled to the test temperature at a rate of 2°C/min. Then it is trimmed using a heated spatula. Afterwards, the gap is decreased to exactly 2.0 mm. Before starting the test, the sample should achieve the correct temperature, and this period is referred to as the equilibration period (30 min). The dynamic data (complex shear modulus, phase angle and complex shear viscosity) were collected over a range of temperatures and frequencies (e.g. 5 to 60°C with temperature intervals of 10°C and 0.1, 0.1259, 0.1585, 0.1995, 0.2512, 0.3162, 0.3981, 0.5012, 0.631, 0.7943, 1.0, 1.259, 1.585, 1.995, 2.512, 3.162, 3.981, 5.012, 6.31, 7.943 and 10 Hz).

RESULTS AND DISCUSSION

Modelling G* using Multi-Linear Regression Models (G*-MLRM)

The regression modelling is the statistical process used

Table 3. Correlation matrix of the independent variables for Nasiriyah asphalt binder.

Correlations factors matrix		G	T	F	PA	DSV	S	St
Pearson correlation	G	1.000	-0.643	0.984	-0.858	-0.840	1.000	-0.168
	T	-0.643	1.000	-0.548	0.819	0.820	-0.642	0.194
	F	0.984	-0.548	1.000	-0.775	-0.750	0.985	-0.149
	PA	-0.858	0.819	-0.775	1.000	0.997	-0.858	0.190
	DSV	-0.840	0.820	-0.750	0.997	1.000	-0.840	0.192
	S	1.000	-0.642	0.985	-0.858	-0.840	1.000	-0.167
	St	-0.168	0.194	-0.149	0.190	0.192	-0.167	1.000
Sig. (1-tailed)	G	.	0.000	0.000	0.000	0.000	0.000	0.071
	T	0.000	.	0.000	0.000	0.000	0.000	0.044
	F	0.000	0.000	.	0.000	0.000	0.000	0.096
	PA	0.000	0.000	0.000	.	0.000	0.000	0.048
	DSV	0.000	0.000	0.000	0.000	.	0.000	0.046
	S	0.000	0.000	0.000	0.000	0.000	.	0.072
	St	0.071	0.044	0.096	0.048	0.046	0.072	.
N	G	78	78	78	78	78	78	78
	T	78	78	78	78	78	78	78
	F	78	78	78	78	78	78	78
	PA	78	78	78	78	78	78	78
	DSV	78	78	78	78	78	78	78
	S	78	78	78	78	78	78	78
	St	78	78	78	78	78	78	78

Where: G= Complex shear modulus (Pa), T=test temperature (℃), F=frequency (Hz), PA=phase angle (°), CSV= dynamic shear modulus (Pa.s), S= shear stress (Pa) and St= shear strain (%).

to determine the relationship between two or more variables to generate a model that predicts one variable from the other(s) in order to present the data in the best fit. The goal of multiple linear regressions is to develop the best model at selected confidence level and satisfying the basic assumptions of regression analysis (Wright and Nocedal, 1999):

i) High inter-correlation does not exist among predictor variables,
ii) Influential observation or outliers do not exist in the data,
iii) The distribution of error is normal,
iv) The mean of error distribution is equal to zero,
v) Errors have a constant variance σ^2 (Homoscedasticity hypothesis).

In order to check if the necessary conditions for the application of MLR are valid for the raw data, we compute the correlation matrix to determine that the independent variables are mutually independent. In the ideal case, the correlation matrix should be an identity matrix (only ones on the main diagonal and zeros elsewhere) (Pallant, 2010). The correlation matrix of the independent variables of the data set can be computed and the result is as given in Table 3. It can be noticed from Table 3 that:

a) The main factor affecting the G* is the applied frequency (higher correction factor in correlation matrix); from the experimental results, a positive relationship between G* and frequency is seen.
b) The second factor is temperature: temperature is a very important parameter affecting the viscosity of asphalt binder; when test temperature increased, viscosity of asphalt binder reduced and then reduced complex shear modulus; it can be seen that there is an inverse relation between them.
c) The third factor is dynamic shear viscosity: when the viscosity of asphalt binder reduced at high temperature or at low frequency, the complex shear modulus reduced too.
d) Phase angle parameter represents the relation between viscous part and elastic part; when the phase angle approaches zero, that means an increase of the elastic part and so that increases complex shear modulus and vice versa when approaching 90°.
e) Shear stress and strain: according to experimental results, we note there is limited impact of shear stress and strain because the test occurs under constant stress or strain mode.

Table 4. Stepwise regression result for average G*.

Asphalt binder	G* predicted=constant +a(T)+b(F)+c(δ)+d(η)+e(σ)+f(ε)									
	Constant	**a**	**b**	**c**	**d**	**e**	**f**	**R^2**	**adj R^2**	**SEE**
Nasiriyah	69967	37	-25978	811	0.01	104.93	-143483	0-91	0-90	0-95
Durah	63251	-3.49	-4997	-647	0.05299	100.56	-30595	0-81	0-80	0-87

Where; G*= Complex shear modulus (Pa), T=test temperature (℃), F=frequency (Hz), δ=phase angle (°), η= dynamic shear modulus (Pa.s), σ= shear stress (Pa) and ε = shear strain (%).

Multiple linear regression models of G* were developed by using the SPSS software version 22 from the result obtained of five samples for each type of asphalt binder. The best and most commonly used method used to determine the parameters of the prediction model is the stepwise method. This method computes the simple regression model for each independent variable (Vapnik and Vapnik, 1998; Pallant, 2010).

The independent variable that has the largest F-value test is chosen as the first variable to be entered. If at least one variable exceeds the standard, the procedure continues. The procedure considers whether the model would be improved by adding a second independent variable and so on. It examines all variables to determine which has the F-value test which suits the selected F-value test as entry criteria. Either F-value test or probability of F-value test are used as entry criteria. Probability of F-value equal to 0.05 was used in the analysis; this corresponds to 3.48 F-value test (Pallant, 2010). A result of the stepwise regression models is given in Table 4.

Bias analysis of models (model validation)

Model validation is strictly an aggregate set of comparisons, and represents the final step in the model development process. The comparison of the applied model in the result of the pure asphalt binder with the observed data serves to indicate how well the model is replicating experimental results. At each step in the model development process, each model component is subjected to a series of validation tests following estimation of the model parameters (coefficients, constants of the model's ability to accurately simulate experimental behaviour).

Data splitting is the act of partitioning available data into two portions for model validation purposes. The first portion of the data, called fitting sample, is used to fit the model and the latter, called validation sample, is used to evaluate its performance. The fitting sample is as large as 75% of the original sample and is extracted from the original sample through a simple random sampling without replacement (the choice of the cut-off point of 75% will be explained later). The remaining data are used as a validation sample. That is, the split is purely random and there is no data duplication (Giancristofaro and Salmaso, 2007).

The statistical validity of G* analysis derived through multiple linear regressions can be assessed by considering the standard statistical tests:

1) The multiple correlation coefficients (R) indicate the degree of association between the independent variable (Y) and the dependent variables (X_1-X_n). This coefficient takes a value between (0) and (1), and the closer it is to (1) the better the linear relationship between the variables. The closer R is to (0) the worse is the linear relationship. The significance of R is that its square (R^2) is approximately the decimal fraction of the variation in the dependent variable (Y) which is accounted for by the independent variables (X_1 to X_n) (Wright and Nocedal, 1999). The formula of R^2 is:

$$R^2 = \frac{SSR}{SST} = \frac{\Sigma(Y-Y\ est)^2}{\Sigma(Y-\bar{y})^2} \quad (19)$$

Where: SSR= Explained variance, and SST= Total variance.

2) The Standard Error of Estimate (SEE) is the square root of the residual mean square. The smaller the value of this statistic, the more precise the predictions will be. The formula of standard error of estimate is:

$$SEE = \frac{\sqrt{\Sigma(Y-Yest)^2}}{N} \quad (20)$$

Where: SEE = Standard Error of Estimate, Y = Observed data used to derive regression equation, e.g. G*, Y_{est} =Value of Y calculated from the regression equation, estimated G*, and N= Total number of samples.

The standard error of estimate is most meaningful when it is expressed as a percentage of the mean observed value of the dependent variable Y (Pallant, 2010) that is,

$$\text{Mean Observed Value}(\%) = \frac{SEE}{\text{Average No. of Samples}} * 100 \quad (21)$$

3) Average Percentage of Error (APE) between predicted

and experimental results was evaluated by using following equation (Ceylan et al., 2008):

$$APE = \frac{\sum_{i=1}^{N}(\varphi_p - \varphi_e)}{N * \varphi_e} \quad (22)$$

Where: φ_p and φ_e are predicted and experimental values.

The average error describes how the model is over-prediction if average error was positive or under-prediction if average error was negative.

4) The (t) test may be used to determine whether an estimated regression coefficient is significant by forming the following ratio:

$$t = \frac{\text{Regression Coefficient}}{\text{Standard Error of The Regression Coefficient}} \quad (23)$$

T-test must be a value of at least (2.0) for significance to be established. Independent variables with a t value of less than (2.0) have no significant relationship with the dependent variable and therefore contribute nothing to the equation. Any such independent variable should be deleted from the equation (Wright and Nocedal, 1999).

5) Line of equality (LQ), which draws a relation between observed and estimated G* for each sample, is the most useful method of evaluating the overall performance of a regression equation. If the points which result from drawing the estimated with experimental G* tend to stand near to the draw line at 45˚, then the resultant model is considered satisfactory. This can be applied by collecting new data, which is the best means of model validation, or splitting data into two sets, the latter of which is used for validation purposes. About 75% of data were used to build G* and 25% were used for the validation process for each sample.

So we need an alternative for MLR in case of complex shear modulus (G*-MLR) because the necessary applications of MLR usually do not hold. These are:

1) Independent variables should be mutually independent of each other.
2) There is a linear relationship between dependent and independent variables.
3) The residuals (the value of errors between the real observed value and the MLR value) should have a normal distribution and should be uncorrelated with the independent variables.

If the conditions for using MLR do not hold, alternative modelling techniques that have less strict conditions are needed. Artificial Neural Network (ANN) is a model-free technique; it is a data-driven technique. ANN does not make rigorous model assumptions like normality, linearity, and independent variables that are mutually independent. This is the reason why ANN is potentially more promising for MLRM (Ozgan, 2011; Bari and Witczak, 2006; Ozgan, 2009; Bishop, 1994).

Modelling complex shear modulus using artificial neural networks (G*-ANN)

Artificial neural network (ANN) is used in an attempt to predict the G* for local asphalt binder. Databases of experimental results of these parameters are used to develop and verify the ANN models. The back-propagation learning algorithm is one of the most important historical developments in neural networks. This learning algorithm is applied to multilayer feed-forward networks consisting of processing elements with continuous and differentiable activation functions. Such networks associated with the back-propagation learning algorithm are also called back-propagation networks. Given a training set of input-output pairs, the algorithm provides a procedure for changing the weights in a back-propagation network to classify the given input patterns correctly. The basis for this weight update algorithm is simply the gradient-descent method as used for simple perceptron with differentiable neurons (Sakhaeifar et al., 2010; Ozgan, 2011).

The input data and the desired output data should be scaled into the range of 0 to 1. The final data-pre-processing step is data balancing. Initially random weights between ±0.5 are assigned to each weight as initial guesses. The weights are learned through an iterative process. During learning, the weights are updated. When the network learns the training set of patterns well enough, it can be used for determining the output values for the pattern with unknown outputs (test period or prediction period).

In this study, MATLAB-2014a Neural Network Toolbox was used for creating the ANN; Multi-Layer Feed-forward Neural Networks and Standard Back Propagation Algorithm were used to train and process the collected data obtained from experimental work (Beale et al., 2010; Demuth et al., 2009).

Model inputs and outputs

An important step in developing ANN models is to select the input variables that have the most significant impact on model performance. A good subset of input variables can substantially improve model performance. Materials' properties, environmental effects, and load-related characteristics of asphalt binder will be chosen as the input and output components for the neural networks' patterns, as these asphalt materials include the complex shear modulus (G*).

The input variables and the output representing (Y) for all cases are shown in Figure 3.

Table 5. Example of input and output statistics for ANN Model for pure Nasiriyah asphalt binder.

Data set	Statistical Parameters	Input variable X1	X2	X3	X4	X5	X6	Output Y
All data	Maximum	50.09	119.10	87.57	390000.00	175100.00	1.24	17620000.00
	Minimum	4.97	0.00	48.65	23550.00	11.82	0.99	1183.00
n=105	Mean	26.00	8.91	69.03	185385.90	29674.08	1.01	2887790.64
	Standard dev.	15.70	19.87	10.57	107474.16	42143.70	0.05	4129392.35
	Range	45.12	119.10	38.92	366450.00	175088.18	0.26	17618817.00
Training	Maximum	50.09	1.25	87.57	390000.00	12000.00	1.12	1203000.00
	Minimum	4.97	0.00	33.55	80400.00	11.82	0.50	1183.00
n=55	Mean	36.18	0.27	76.72	268751.82	3009.16	0.99	300973.04
	Standard dev.	13.44	0.36	8.30	76267.70	3478.54	0.07	348146.75
	Range	45.12	1.25	54.03	309600.00	11988.18	0.62	1201817.00
Testing	Maximum	35.03	3.99	68.94	159000.00	28060.00	1.00	2807000.00
	Minimum	4.98	1.26	62.63	112000.00	12370.00	1.00	1237000.00
n=19	Mean	18.69	2.39	65.77	135281.58	19385.00	1.00	1939500.00
	Standard dev.	10.65	0.88	1.81	15130.66	4933.29	0.00	493126.98
	Range	30.05	2.73	6.31	47000.00	15690.00	0.00	1570000.00
Validation	Maximum	15.00	119.10	58.04	73920.00	175100.00	1.24	17620000.00
	Minimum	4.97	11.91	48.65	23550.00	61670.00	0.99	1183.00
n=31	Mean	10.79	41.57	53.34	48631.58	110067.11	1.07	3699209.27
	Standard dev.	5.07	29.59	3.02	14791.78	31687.42	0.09	5745520.69
	Range	10.03	107.19	9.39	50370.00	113430.00	0.25	17618817.00

Dependent variables: Y ($G^*_{predicted}$): Complex shear modulus (G*) (Pa).

Independent variables: X_1(T): Test temperature (°C),
X_2(f): Frequency (Hz),
X_3(δ): Phase angle (degree, °),
X_4(η): Dynamic shear viscosity (Pa s),
X_5(σ): Shear stress (Pa),
X_6(ε): Shear strain (%).

b) Data division and pre-processing

It is a common practice to divide the experimental data into three sets for the training, testing, and validation stages as is standard practice in the development of ANN models. The set for the training stage is used to adjust the connection weights of the neural network. The set for testing is used to check the performance of the neural network at various stages of learning, and training is stopped once the error in the testing set increases. The set for validation is used to evaluate the performance of the model once training has been successfully accomplished.

A trial and error process was used to select the best division. In the current study, the network that performs best with respect to testing error was used and compared with other criteria to evaluate the prediction performance, testing error and correlation of validation set. Using the default and non-default parameters of the software, a number of networks with different division were developed and the result showed that 70% of the data are used for training and 30% are used for testing and validation. The training data are further divided into 70% for the training set and 30% for the testing set (the total data are 105 divided into 74 points (divided into 55 for training and 19 for testing) and 31 points for the validation stage).

The effect of using different distribution of data (that is, striped, blocked, and random) is investigated and shows that the best performance is obtained when the random choice is used.

The statistical parameters are considered to include the maximum, minimum, mean, standard deviation and variable range. The statistics of the training, testing and validation sets for the ANN models are shown in Table 5.

To examine how representative the training, testing and validation sets are with respect to each other, t-test and F-value test are carried out. The t-test examines the null

Table 6. Null hypothesis test for ANN input variable and outputs.

Variable and data set	T-value	Lower critical value	Upper critical value	t-test	F-value	Lower critical value	Upper critical value	F-value test
X1								
Testing	-0.42	-1.96	1.96	Accept	1	0.86	1.17	Accept
Validation	-0.29	-1.96	1.96	Reject	1	0.85	1.19	Reject
X2								
Testing	-2.14	-1.96	1.96	Accept	1.98	0.86	1.17	Accept
Validation	-2.14	-1.96	1.96	Accept	1.98	0.85	1.19	Accept
X3								
Testing	-0.18	-1.96	1.96	Accept	0.94	0.86	1.17	Accept
Validation	-0.41	-1.96	1.96	Accept	0.94	0.85	1.19	Accept
X4								
Testing	-0.35	-1.96	1.96	Accept	0.96	0.86	1.17	Accept
Validation	-0.32	-1.96	1.96	Accept	0.93	0.85	1.19	Accept
X5								
Testing	-0.11	-1.96	1.96	Accept	0.95	0.86	1.17	Accept
Validation	0.04	-1.96	1.96	Accept	0.96	0.85	1.19	Accept
X6								
Testing	0.18	-1.96	1.96	Accept	0.98	0.86	1.17	Accept
Validation	-0.13	-1.96	1.96	Accept	0.95	0.85	1.19	Accept
Y								
Testing	0.09	-1.96	1.96	Accept	0.92	0.86	1.17	Accept
Validation	-0.17	-1.96	1.96	Accept	0.89	0.85	1.19	Accept

hypothesis of no significant difference in the means of the two data sets and the F-value test examines the null hypothesis of no difference in the variances of the two sets. For a given level of significance, test statistics can be calculated to test the null hypotheses for the t-test and F-value test respectively. Traditionally, a level of significance equal to 0.05 is selected. This means that there is a confidence level of (95%). The results of the t-test and F-value tests are given in Table 6.

C) Model architecture

The predicted complex shear modulus can be derived based on the training set. The number of hidden nodes determines the ANN model.

There is a rule of thumb for the number of hidden nodes (Bishop, 1994) using Equation 24:

$$\text{Number of hidden nodes} = \sqrt{m * n} \qquad (24)$$

Where: m is the number of output neurons, and n is the number of input neurons.

So, in this study the number of hidden nodes = $\sqrt{1 * 6}$ = 2.45, so 3 hidden nodes are used.

Results analysis

Predicted G of pure Asphalt binder*

The relation between the experimental and predicted complex shear modulus by ANN and MLRM is demonstrated in Figures 5 and 6 for Nasiriyah and Durah asphalt binder respectively. It is noticed from the value of R^2 that the G*-ANN model is better at predicting than G*-MLRM. Trend line for the results obtained from multi-linear regression is far away from the equality line; that means the prediction data from this model are not presenting real experimental results, but the trend line that is obtained from the ANN result is near the equality

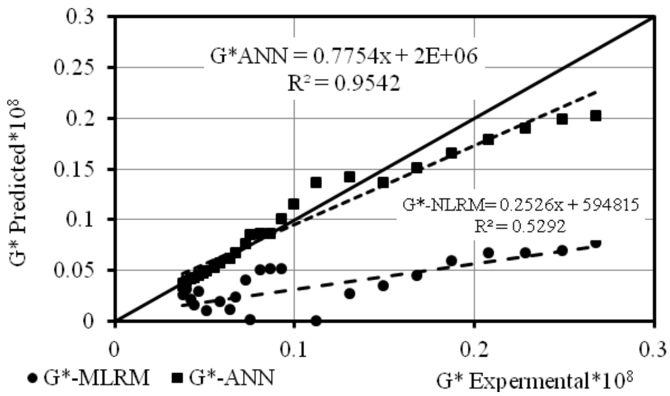

Figure 5. Experimental against predicated G* of ANN and MLRM for pure Nasiriyah asphalt binder.

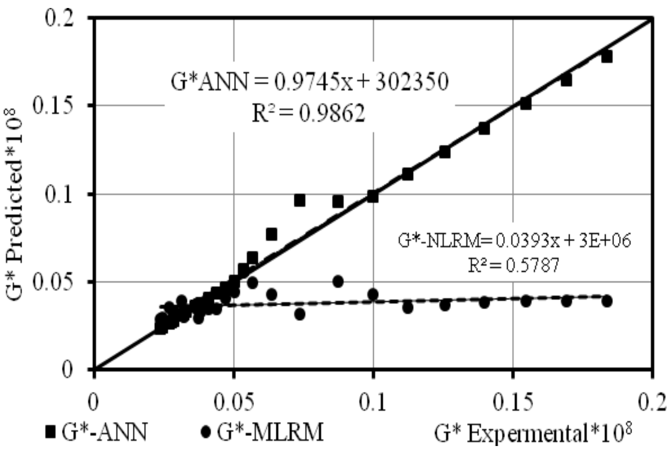

Figure 6. Experimental against predicated G* of ANN and MLRM for pure Durah asphalt binder.

line and gives more accuracy when predicting the value of G*.

Predicted G of modified Asphalt binder*

Neural network technique was used for simulating and predicting the G* of modified asphalt binder tested in DSR. Two types of styrene-butadiene-styrene (SBS) at three different modification levels, namely 3, 6 and 9%, by weight of the bitumen were used to modify the local asphalt binder and the results are as shown in Figures 7 and 8.

Error analysis of models

Figure 9 summarises the average percentage of error for ANN and MLRM for G*. It can be noticed that the ANN model is under-prediction for Durah asphalt binder while it is over-prediction for Nasiriyah asphalt binder, as shown from the negative and positive average percentage error. In addition, the ANN model's prediction for G* has a lower tendency towards this bias than MLRM due to lower average percentage of error.

Figure 10 explains the average percentage of error for developed G*-ANN based on the pure asphalt binder which is used to predict complex shear modulus. It can notice that:

i) The developed G*-ANN model can be used to simulate the modified asphalt binder;
ii) Adding SBS in both types modified rheological properties of asphalt binder (enhanced viscosity and then increased ability of asphalt binder to resist shear deformation; in other words, increased experimental complex shear modulus);
iii) The predicted G* in most cases over-estimated the experimental result but within a suitable range not greater than 5%.

Conclusion

The following conclusions were obtained based on the experimental results and discussion:

i) The main factors that affect the G* from the result of correlation matrix analysis are frequency, dynamic shear viscosity, phase angle and temperature.
ii) Experimental results of amplitude sweep test for asphalt samples were tested in DSR for evolution of the ANN model to predict G* of asphalt binder; these ANN models were based on basic parameters, temp., frequency, dynamic shear viscosity, phase angle, shear stress and strain to be independent variables of the ANN model. The results revealed that the correction between predicted and experimental was excellent for both types of asphalt binders.
iii) Bias analysis for all predicted models (ANN and MLRM) was evaluated based on the values for the line of equality because it is considered to be a better model than average percentage error. The result analysis stated that the ANN model is the nearest to line of equality because it had a lower bias for error percentage.
iv) The architectures of ANN models were determined after investigating several architectures containing one to three hidden layers with six neurons in each hidden layer. The best ANN model was three hidden layers with six neurons based on the high R^2 between experimental and predicted results.

Conflict of Interest

The author did not declare any conflict of interests.

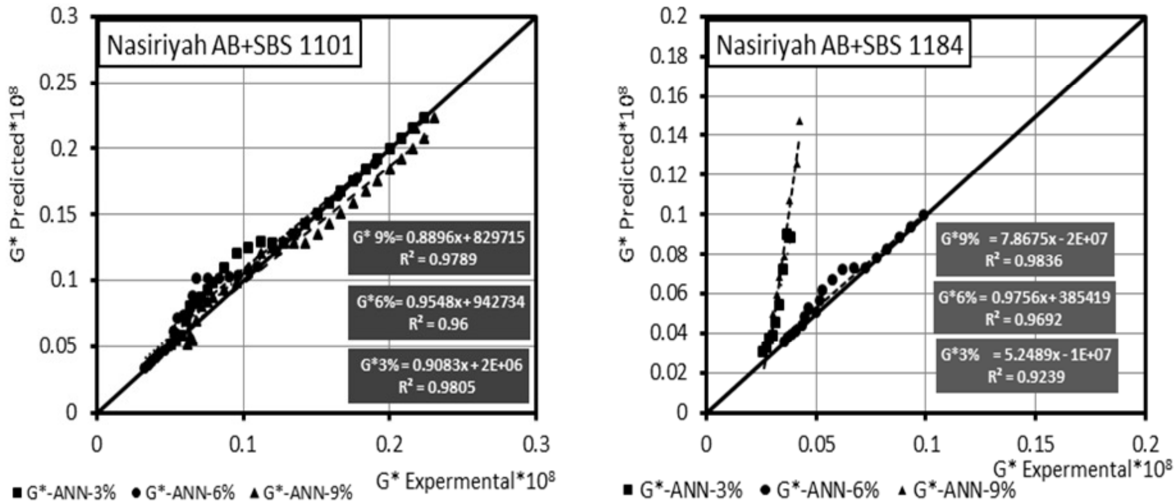

Figure 7. Experimental against predicated G* of ANN and MLRM for pure Modified Nasiriyah AB.

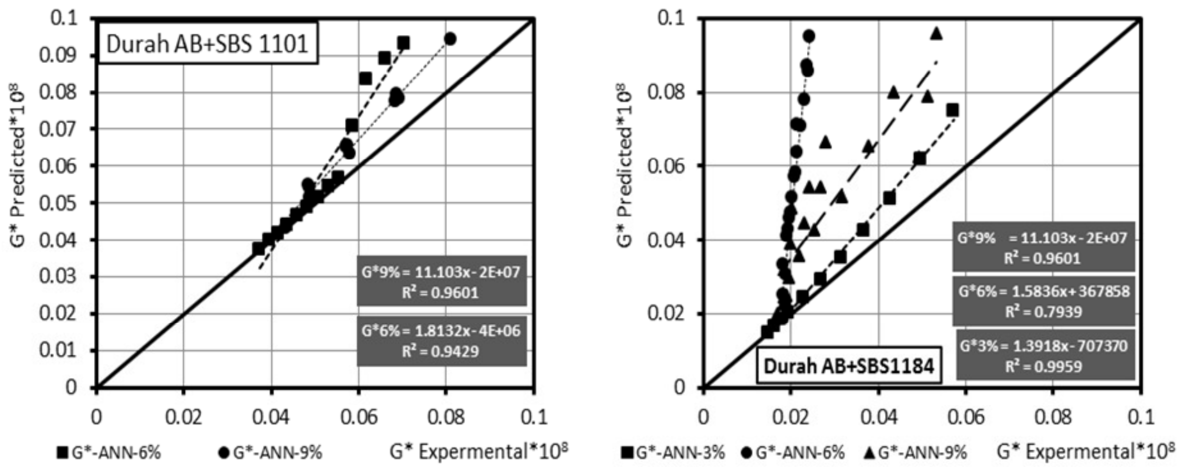

Figure 8. Experimental against predicated G* of ANN and MLRM for pure Modified Durah AB.

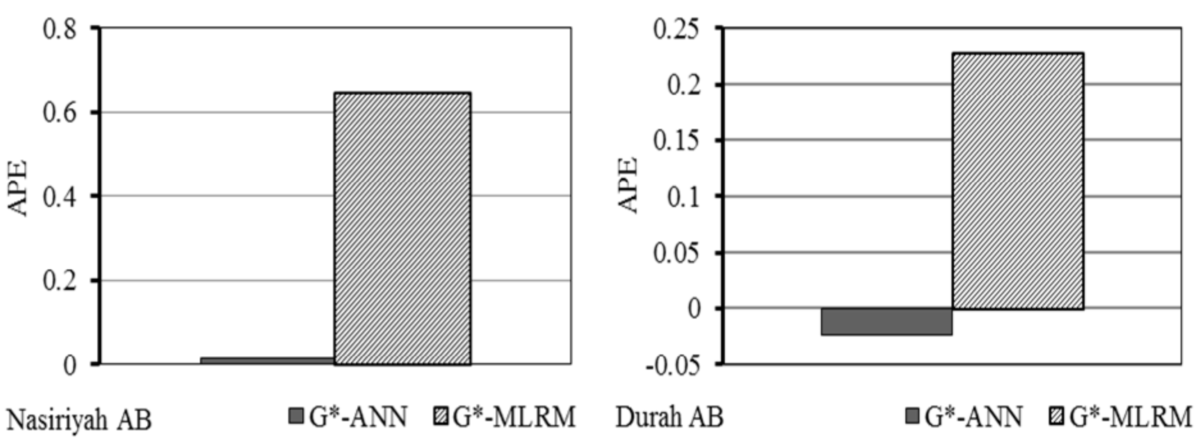

Figure 9. APE of ANN and MLRM of G* for pure asphalt binder.

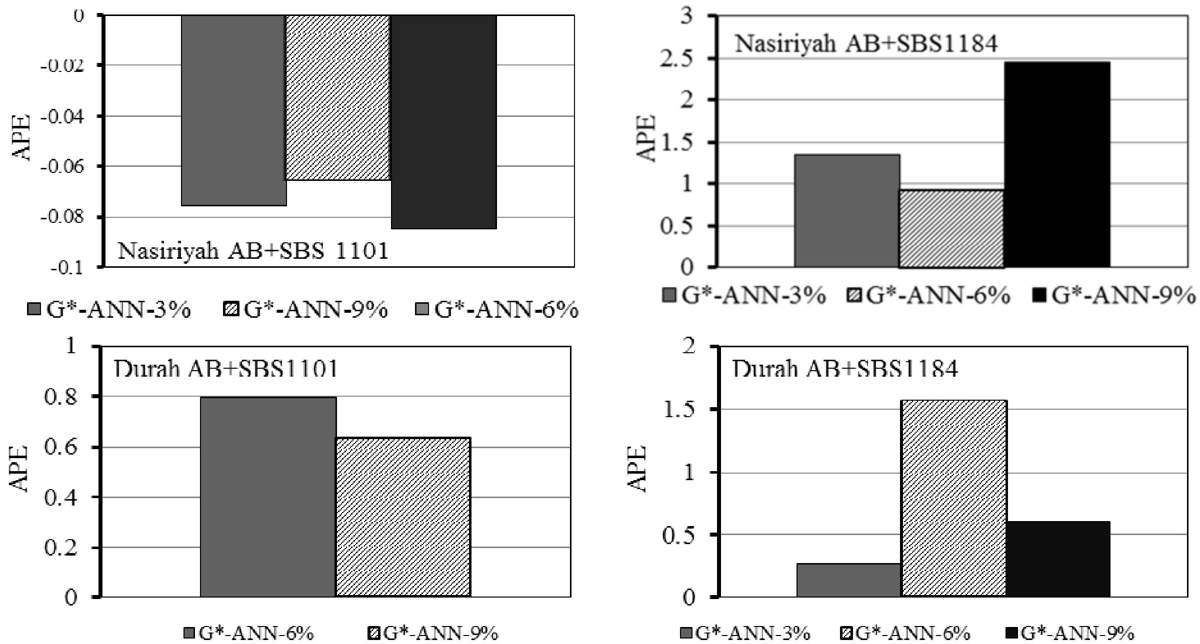

Figure 10. APE of ANN and MLRM of G* for modified asphalt binder.

ACKNOWLEDGEMENT

The author sincerely thanks Dr Hussain A. Khalid at the University of Liverpool for allowing the use of DSR to evaluate the local asphalt binders.

REFERENCES

Bari J, Witczak MW (2006). Development of a New Revised Version of the Witczak E* Predictive Model for Hot Mix Asphalt Mixtures (With Discussion)." J. Assoc. Asphalt Paving Technol. P. 75.

Beale MH, Hagan MT, Demuth HB (2010). Neural Network Toolbox 7." User's Guide, MathWorks.

Bishop CM (1994). Neural networks and their applications. Rev. Scient. Instrum. 65(6):1803-1832. http://dx.doi.org/10.1063/1.1144830

Ceylan H, Gopalakrishnan K, Kim S (2008). Advanced Approaches to Hot-Mix Asphalt Dynamic Modulus Prediction. Can. J. Civil Eng. 35(7):699-707. http://dx.doi.org/10.1139/L08-016

Demuth H, Beale M, Hagan M (2009). Neural network toolbox user's guide, The MathWorks." Inc., Natrick, USA.

Giancristofaro RA, Salmaso L (2007). Model Performance Analysis and Model Validation in Logistic Regression. Statistica 63(2):375-396.

Goodrich JL (1988). Asphalt and polymer modified Asphalt properties related to the performance of Asphalt concrete mixes (with discussion). Association of Asphalt Paving Technologists Proc.

Lytton RL, Uzan J, Fernando EG, Roque R, Hiltunen D, Stoffels SM (1993). Development and Validation of Performance Prediction Models and Specifications for Asphalt Binders and Paving Mixes, Strategic Highway Research Program.

Ozgan E (2009). Fuzzy logic and Statistical-Based Modelling of the Marshall Stability of Asphalt Concrete under Varying Temperatures and Exposure Times." Advan. Eng. Software 40(7):527-534.

Ozgan E (2011). Artificial Neural Network Based Modelling of the Marshall Stability of Asphalt Concrete." Expert Syst. Appl. 38(5):6025-6030.

Pallant J (2010). SPSS Survival Manual: A Step by Step Guide to Data Analysis using SPSS, McGraw-Hill International.

Poulikakos LD, Partl M (2012). A Multi-Scale Fundamental Investigation of Moisture Induced Deterioration of Porous Asphalt Concrete, Constr. Build. Mater. 36:1025-1035. http://dx.doi.org/10.1016/j.conbuildmat.2012.04.071

Priddy KL, Keller PE (2005). Artificial neural networks: an introduction, SPIE Press. http://dx.doi.org/10.1117/3.633187; PMCid:PMC2253434

Sakhaeifar MS, Underwood BS, Kim YR, Puccinelli J, Jackson N (2010). Development of Artificial Neural Network Predictive Models for Populating Dynamic Moduli of Long-Term Pavement Performance Sections." Transportation Research Record: J. Transport. Res. Board. 2181(1):88-97. http://dx.doi.org/10.3141/2181-10

Vapnik VN, Vapnik V (1998). Statistical learning theory, Wiley New York.

Wright S, Nocedal J (1999). Numerical Optimization, Springer New York.

academicJournals

Vol. 6(3), pp. 27-50, April 2015
DOI: 10.5897/JCECT2015.0356
Articles Number: 2961AE452271
ISSN 2141-2634

http://www.academicjournals.org/JCECT

Journal of Civil Engineering and Construction Technology

Full Length Research Paper

Fatigue evaluation of Iraqi asphalt binders based on the dissipated energy and viscoelastic continuum damage (VECD) approaches

Abdulhaq H. A. A. Al-Haddad

School of Engineering, University of Liverpool, Liverpool, United Kingdom.
The University of Mustansiriyah; Engineering College, Highway and Transportation Dept., Baghdad, Iraq.

Received 29 January, 2015; Accepted 25 March, 2015

Bituminous materials in roads are subjected to short-term loading each time a vehicle passes. If sufficiently high, the loading results in a loss of rigidity of the material and can, by accumulation in the long term, lead to failure. The resulting fatigue deterioration is of great importance in pavement construction and must be correctly understood in order to ensure adequate structural design. The binder property plays a major role in determining the mechanical characteristics in asphalt pavement to resist distress. This paper presents results of an investigation to evaluate the effects of fume silica, ground slug and two types of styrene-butadiene-styrene (SBS) on the fatigue performance of local bituminous binders. These additives were incorporated into asphalt binder from two different sources, namely Nasiriyah and Durah refinery in the middle and southern regions of Iraq. This study adopts a time sweep (TS) test method to study the fatigue phenomenon under controlled strain and stress modes using a dynamic shear rheometer (DSR). Fatigue life of the asphalt binder is defined using the traditional approach based on number of cycles required to cause to failure and reduction in initial stiffness. To accurately predict the fatigue life of modified and unmodified binders, the viscoelastic continuum damage (VECD) approach and energy approach have been also adopted. It was found that additives had a superior performance in terms of fatigue life. However, the energy approach has been shown to be more realistic in predicting the fatigue life of modified binders than the VECD approach as the latter did not correlate well with traditional and energy approaches. It can be concluded that the fatigue performance of Durah asphalt binder is better than that of Nasiriyah in all cases with or without adding additives. Adding 2% silica fume and 6% SBS 1184 enhanced the fatigue performance of local asphalt.

Key words: Asphalt binder, fatigue performance, time sweep test, viscoelastic continuum damage (VECD), dissipated energy, plateau value, energy ratio, and energy stiffness ratio.

INTRODUCTION

Flexible pavements are designed to resist rutting, fatigue, low temperature cracking and other distresses. The most serious distresses associated with flexible pavement are cracking, which occurs at intermediate and low

*Corresponding author. E-mail: Abdulhaq@liverpool.ac.uk.

temperatures, and permanent deformation, which occurs at high temperatures. These distresses reduce the service life of the pavement and increase the maintenance costs. Bituminous binder plays an important role in the behaviour of pavement structures. It influences various deterioration modes. It has been reported that binder influences asphalt distress by approximately 60% in terms of fatigue crack (Harvey and Cebon, 2003). In fact, fatigue is one of the main types of asphalt pavement deterioration. In reality, fatigue life is defined as the number of standard axles passing until mechanical failure while, in the laboratory, it is defined as the number of stress or strain cycles to failure of a sample predicted by fatigue criteria. Asphalt cement binds the aggregate particles together, enhancing the stability of the mixture and providing resistance to deformation under induced tensile, compressive and shear stresses. Bitumen materials are viscoelastic and their mechanical behaviour is dependent on both the temperature and rate of loading. At low temperatures and short loading times, asphalt cements behave as elastic solids, while at high temperatures and long loading times they behave as simple viscous liquids. At intermediate temperatures and loading times, the behaviour is more complex. A medium temperature range from 15 to 30°C is most suitable for fatigue cracking analysis and pavement fatigue life prediction (Deacon et al., 1994).

Several papers have been published that used a dynamic shear rheometer (DSR) to investigate binder fatigue properties (Bahia et al., 1999; Sybilski et al., 2013). In these papers fatigue is measured by continuing load cycles until a decrease in the evolution of the complex shear modulus G* versus loading time occurs. Bahia et al. (1999) used the plate-plate set-up, while Phillips (1998) used cone-plate geometry. Bahia et al. (1999) conducted tests in the linear and also in the nonlinear range of viscoelasticity with a fixed number of load cycles (5,000 or 11,000 with strains of 1, 10, 20 and 50%). Material failure was defined by the amount of the reduction of G*. In these studies, estimation and measurement of asphalt healing was also considered. It was shown that both strain dependency and fatigue are highly sensitive to the composition of the binders, the type of additives, the temperature, the heating rate, the aging process and the interaction of these factors. A significant improvement of fatigue properties can be achieved through binder modification with polymers. The papers indicate that high strain testing and determination of nonlinear properties are essential for understanding the mechanical role of binders in asphalt mixtures.

Within the last decade many research centres have started studies on binder fatigue phenomena (Bahia et al., 2001; Bonnetti et al., 2002; Anderson et al., 2001; Nicholls, 2006; Airey et al., 2004).

The goals are multiple, e.g.:

1. Understand the binder component affecting the Fatigue of the asphalt binder,
2. Be able to measure fatigue behavior of the binder itself, and
3. Evaluate the influence of binder modifications or additives.

NCHRP Project 9-10 (Superpave Protocols for Modified Asphalt Binders) identified the general lack of correlation between mixture fatigue performance and [$G^* \sin\delta$]; therefore, the development of improved binder fatigue testing procedures has been pursued. During NCHRP 9-10, the time-sweep (TS) test was introduced as a binder-specific fatigue test performed in the DSR, where the specimen is subjected to repeated cyclic shear loading in either controlled-stress or controlled-strain mode at constant amplitude to measure the fatigue life of asphalt binders (Bahia et al., 2000; Bonnetti et al., 2002). The TS test allowed for the binder to go beyond linear viscoelastic behavior and into the damage accumulation range. Results from this testing gave a much higher correlation with mixture fatigue performance ($R^2 = 0.84$), indicating that the TS test was a promising procedure for evaluating binder fatigue characteristics.

Fatigue cracking and permanent deformation are considered to be the most serious distresses associated with flexible pavements. To reduce the pavement distresses, there are different solutions such as adopting a new mix design or by using asphalt additives. Use of asphalt additives in highway construction is known to give the conventional bitumen better engineering properties as well as being helpful to extend the lifespan of asphalt concrete pavement.

Polymer is a common method used to modify bitumen and addition of polymers has gained popularity in recent years. This is because modification provides the diversified properties needed to build better-performing roads. Polymeric modifiers have been introduced as a potential source of specific improvements in the characteristics of asphalt binder and mixtures. The main reasons that asphalt modification has become more accepted are the traffic factors, which have increased, including heavier loads, higher volumes and higher tyre pressures. Zhu et al. (2014) defined asphalt modifier as a material that, would normally be added to the binder or the mixtures to improve its properties. The choice of modifier for a particular project can depend on many factors including construction ability, availability, cost, and expected performance. Khodary (2010) described that the technical reasons for using modifiers in asphalt concrete mixtures are to produce stiffer mixes at high service temperature to resist rutting as well as to obtain softer mixtures at low temperature to minimise thermal crack and improve fatigue resistance of asphalt pavement. Improvement in the performance of asphalt concrete mixtures that contain polymer is largely due to the improvement in the rheological properties of the asphalt binder. The rheological properties of a binder that

Table 1. Properties of the asphalt binder.

Property	Nasiriyah	Durah
Penetration (0.1 mm, 100 g and 5 s)- ASTM D5	41	43
Softening point (°C) - ASTM D36	52	53
Penetration Index(PI)	-1.0	-0.35
Viscosity cP, 135°C) ASTM D 4402	500	481.3

Table 2. Chemical properties of GG.

Parameter	Principal oxides (%)				
	CaO	SiO_2	Al_2O_3	MgO	Fe_2O_3
Regen company*	40	35	12	10	0.2
Portland cement	65	20	5	1	2

Regen Ground Granulated Blast furnace Slag (GGBS) is a cement substitute, manufactured from a by-product of the iron-making industry. The use of Regen in concrete reduces embodied CO_2 emissions by over 900kg per tonne of cement, and also increases its durability. http://www.heidelbergcement.com/uk/en/hanson/products/cements/ggbs_and_related_products/regen_ggbs.htm

allow flexibility under load control resistance to fatigue. The modified mixtures are less brittle at lower temperatures and have higher stiffness at higher temperatures compared to normal mixtures. This makes polymer modification extremely attractive for pavement designers and highway agencies.

Asphalt is exposed to a wide range of load and weather conditions; however, it does not have good engineering properties, because it is soft in a hot environment and brittle in cold weather. Therefore, asphalt is usually reinforced by polymers to improve its mechanical properties. The main advantage of using modified bitumen is the effect on the pavement performance in terms of permanent deformation. In the previous studies, it was recorded that 2 to 6 wt. % of SBS in bitumen should be used to improve the properties of base bitumen significantly (Isacsson and Lu, 1995). In this investigation, 3 and 6 wt. % SBS in bitumen were used for bitumen modification.

Objectives of the study

The objectives of this study were to:

1. To assess the fatigue behavior for the local asphalt and modify it using polymers.
2. To predict fatigue life of local asphalt binder in order to use it in pavement design.

EXPERIMENT

Materials

In this research, an investigation was made into the fundamental studies of modified asphalt binder and mixtures in order to understand the influence of modifiers on the rheological properties and fatigue resistance with the aim of preventing fatigue cracking in asphalt pavement. The conventional bitumen samples were acquired from two sources (Nasiriyah and Durah refineries) which are commonly used in the middle and south of Iraq, with (40-50) penetration grade and which are expected to have different fatigue life capacities, modified with microsilica (s), ground granulated blast furnace slag (GG) and two types of styrene-butadiene-styrene (SBS) at three different modification levels, namely 3, 6 and 9% by weight of the bitumen. It is worth noting that, for the purpose of identifying fundamental fatigue performance of modified bituminous binder, an original modified binder with no ageing effect was considered in this study. The properties of asphalt binders and additives are shown in Tables 1 to 4.

Sample preparation and test conditions

The asphalt binder was preheated in an oven to the recommended temperature (160 ± 5°C) for the unmodified binders and (160 ± 5°C) for the modified binders, but one should note that binders were just heated up for a certain time to soften them to prevent ageing. Samples should be stirred before pouring into a silicon mould (stirring may be done manually) as the received sample must be homogenised when it is poured in the mould. Moulds should be left at room temperature (from 18 to 24°C) to cool the sample. Silicon moulds are then used to prepare samples for amplitude sweep and fatigue tests, as seen in Figure 1a to e. Both amplitude sweep and fatigue tests were conducted with the 8 mm plate-plate set-up. All tests were conducted at a frequency of 10 Hz, using 2 mm gap settings and the test temperature was 25°C.

The sample is loaded into the rheometer within 60 min of moulding. The temperature of the rheometer plates during loading should be high enough in order to assure good adhesion to the plates. In the case of unmodified binders, a 60°C temperature is recommended. In any case, the sample should start flowing to get good adhesion to both plates (the gap is first decreased to 2.05 mm). The sample is cooled to the test temperature (25°C is recommended in this work) at a rate of 2°C/min. Then it is trimmed using a heated spatula. Afterwards, the gap is decreased to exactly 2.0 mm. Before starting the fatigue tests, the sample should

Table 3. Summary properties of elastomer used (Kraton Polymers, 2006).

Property	D 1101 K SBS	D 1184 K SBS
Tensile strength (PSI).	4,600	4,000
Elongation (%)	880	820
Specific gravity	0.94	0.94
Brookfield Viscosity (cps at 77°F)	4,000	20,000
Diblock (%)	16%	16%
300% modulus (PSI)	400	800
Molecular structure	Linear	Radial

Table 4. Properties of Elkem Microsilica Grade 940.

Chemical and physical requirements	Specification (characteristic values)
SiO_2 (%)	> 90
H_2O (moisture content when packed, %)	> 90
Loss on Ignition, LOI (%)	< 3.0
Retained on 45 micron sieve (tested on Undensified, %)	< 1.5
Bulk density - undensified (when packed, kg/m^3).	200 - 350
Bulk density - densified (when packed, kg/m^3).	500 - 700

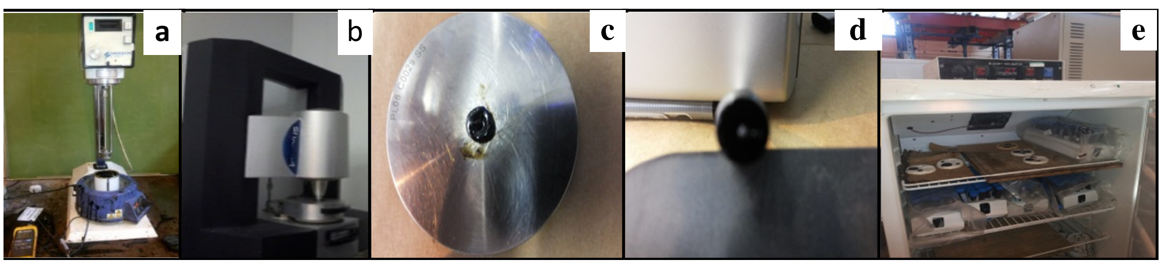

Figure 1. (a) Shear mixer (b) Kinexus Pro$^+$ DSR (c) steel plate, (d) spindle after failure (e) silicon moulds in fridge.

achieve the correct temperature, and this period is referred to as the equilibration period. An equilibration period of 30 min is recommended at the test temperature of 25°C. During the equilibration period the sample modulus can be tested at a very low strain level every 3 min (at least 10 measuring points should be obtained before starting the fatigue test).

Mechanical testing

Stress-strain amplitude determination

The stress or strain levels for the experimental work were selected from the experimental results of amplitude sweep stress and strain used in establishing the linear viscoelastic regions of the asphalt binders. It was defined that the LVER (Linear Visco Elastic Regain) limit is the point at which the modulus decreased to 95% of the initial shear modulus.

A single stress and strain level for asphalt binders were chosen respectively within in the LVER limit in order to reduce the testing time of fatigue test. Tests were conducted at 25°C and three replicates were performed for each condition. Figure 2 illustrates an example of sweep strain and stress for Nasiriyah asphalt binder. It should be mentioned that sweep stress and strain were just conducted on pure asphalt binders, and then the selected strain and stress values were implanted on all bitumen samples (pure and modified) so that comparison could be made with the control binder. Table 5 summarises the selected controlled strain and stress values for both binder grades.

Binder fatigue test

In general, there are two different approaches for studying the fatigue behavior of the asphalt binder. These can be broadly classified into phenomenological (empirical) approaches and mechanistic approaches. The phenomenological approaches are completely based on experimental data and are popular among engineering communities due to their simplistic nature. On the other hand, mechanistic approaches are based on fundamental energy, mechanics-based principles, and are complex but applicable to a wide range of loading and environmental conditions. The phenomenological models relate the fatigue performance to the properties of asphalt concrete in an undamaged state. However, damage evolution in asphalt concrete is complicated due to interaction among viscoelastic effects, relaxation, healing and the heterogeneous nature of the mix.

In this study, binder fatigue tests were conducted using the

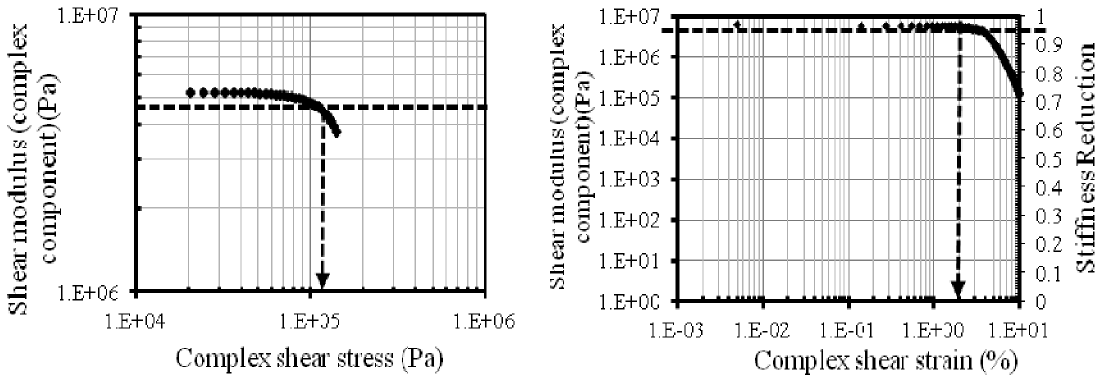

Figure 2. Sweep stress and sweep strain for Nasiriyah asphalt binder.

Table 5. Levels of stress and strain used in fatigue tests.

Binder source	Stress level, Pa	Strain, %
Nasiriyah refinery	120000-150000	2.0
Durah refinery	100000-120000	2.5

Kinexus Pro+ DSR developed by the Malvern Instrument Company, as shown in Figure 1b. The details of test conditions are as follows:

1. Both controlled stress and strain mode were conducted,
2. A high frequency 10 Hz is recommended to reduce testing time and number of load cycles,
3. It is recommended to perform the test at stress and strain levels within the LVER.

It is recommended that the fatigue test is performed:

1. Until the binder stiffness modulus G* reaches 20 and 50% of the initial value,
2. Due to differences in fatigue behavior of modified and unmodified bitumen, it is recommended to gather test results allowing for the analysis of the results with a conventional as well as a dissipated energy approach (energy ratio (ER); reduced dissipated energy change (RDEC), plateau value (PV) and energy stiffness ratio (ESR)),
3. Applied viscoelastic continuum damage to assessment damage in asphalt binder,
4. Previous researchers recommended conducting fatigue tests using DSR at relatively low temperature in order to minimise the edge effect in the parallel plate of the DSR as a heterogeneous flow (plastic flow) may accrue at high temperature. In fact, the sophisticated Kinexus Pro+ DSR has the ability to overcome this issue because of machine capacity. This DSR incorporates controlled hood temperature which keeps a uniform temperature during the test. The test temperature used in this work was chosen as 25°C, as this is similar to the middle and southern regions of Iraq,
5. After performing the fatigue test, it is strongly recommended to check the bottom and the upper plate; if the test is performed correctly, both plates should be covered with bitumen when the fatigue test is finished. If this is not the case, the adhesion between the plate and the binder was probably not sufficient, and the test needs to be repeated, and the temperature at which the binder is loaded into the DSR can be increased, as shown in Figure 1b.

RESULTS AND DISCUSSION

Conventional approach

Conventional fatigue criteria defining fatigue life of the asphalt binder are arbitrary criteria which consider only stiffness modulus instead of the overall material properties. It is also worth noting that, for higher temperatures and loads, a decrease of stiffness modulus at the beginning of the test is significant and not always exclusively connected to the fatigue phenomenon. Conventional fatigue criteria, define failure of a material as a situation when its stiffness modulus decreases to 50% of its initial value for strain mode operation, whereas, in the controlled stress mode, it is defined as a reduction of stiffness modulus of the sample to 10% of its initial value (Artamendi and Khalid, 2005) or a complete fracture of the sample (Ghuzlan and Carpenter, 2006). In this study, for strain mode, failure criteria of 20 and 50% reduction in stiffness modulus of initial value and 10% for stress mode were adopted. Increased Fatigue Life Ratio (IFLR) parameters are calculated for each case as ratio of number of cycles caused to required failure criteria (50, 20 and 10%) between modified and unmodified (pure) asphalt in order to compare the results. The coefficient of variance on number of cycles at 20 and 50% reduction in shear modulus (strain mode) and to 10% reduction in shear modulus (stress mode) was also calculated. In all cases it can be said that it is acceptable, as shown in Figure 3 and Table 6.

In all cases in Figures A1, 5, 9 and 13 in the Appendix; it can be seen that:

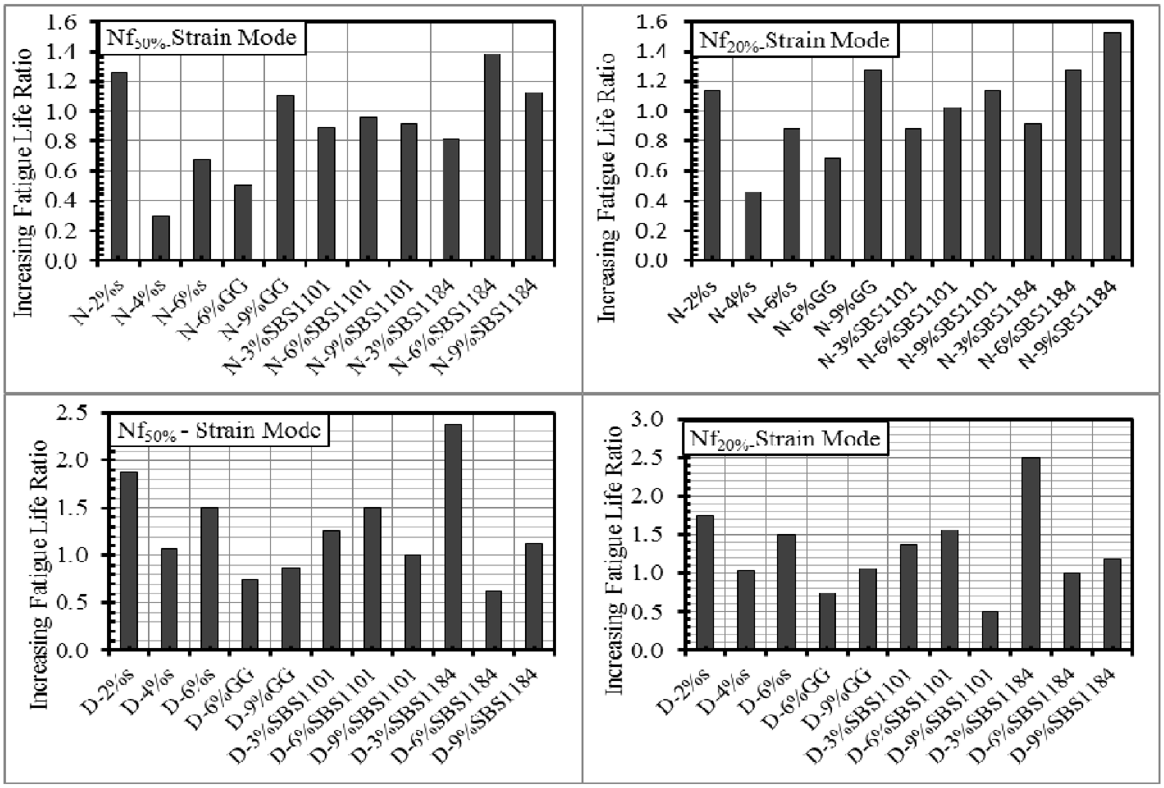

Figure 3. IFLR for the conventional approach.

Table 6. Conventional fatigue approach result

Parameter	Av. Increased fatigue life ratio (IFLR) with standard division											
	Nasiriyah Asphalt						Durah Asphalt					
	Strain mode				Stress mode		Strain mode				Stress mode	
	$Nf_{50\%}$	σ	$Nf_{20\%}$	σ	$Nf_{10\%}$	σ	$Nf_{50\%}$	σ	$Nf_{20\%}$	σ	$Nf_{10\%}$	σ
2%s	1.255	1.725	1.136	1.454	5.500	1.799	1.875	1.121	1.750	1.350	1.870	2.471
4%s	0.298	1.020	0.455	0.859	0.875	1.063	1.063	0.517	1.031	0.623	3.304	1.140
6%s	0.681	1.686	0.886	1.421	3.938	1.927	1.500	0.862	1.500	1.038	3.957	1.900
6%GG	0.502	1.137	0.682	0.958	0.375	1.299	0.750	0.690	0.750	0.831	0.609	1.520
9%GG	1.106	1.176	1.273	0.991	0.250	1.344	0.875	1.155	1.063	2.547	1.391	2.547
3%SBS1101	0.894	1.255	0.886	1.057	0.875	1.434	1.250	1.000	1.375	2.205	1.870	2.205
6%SBS1101	0.957	1.608	1.023	1.355	1.313	1.837	1.500	1.034	1.563	2.281	3.304	2.281
9%SBS1101	0.915	0.314	1.136	0.264	2.750	0.358	1.000	1.207	0.500	3.385	3.957	2.661
3%SBS1184	0.809	2.510	0.909	2.115	1.500	2.867	2.375	1.034	2.500	2.901	5.435	2.281
6%SBS1184	1.383	1.294	1.273	1.090	1.563	1.608	0.625	1.207	1.000	3.385	1.739	2.661
9%SBS1184	1.128	1.412	1.523	1.189	1.000	1.754	1.125	1.466	1.188	4.110	1.522	3.231

1. Micro silica significantly increases the fatigue life of asphalt binder regardless of binder sources and test mode. According to Table 1, adding 2% silica is a suitable amount to enhance fatigue performance for both sources of asphalt binder,
2. The IFLR increased when the percentage of GG additives increased,
3. The IFLR increased with increased percentage of additives until 6% and then reduced for both types of SBS. Adding SBS 1184 increased the ability of the asphalt binder to resist fatigue more than adding SBS1101,

4. In more cases, fatigue performance of Durah asphalt binder is better than that of Nasiriyah.

However, in the conventional approach, the fatigue performance is assessed on the number of cycles against the reduction in the shear modulus without taking in account other variables such stress, strain, phase angle. Therefore, within this study, dissipated energy ratio (ER) and viscoelastic continuum damage are adopted (VECD) were adopted which both of them are advanced criteria to assess the fatigue life of bituminous.

Energy approach

Energy ratio method

Once the load is applied to the material, the resulting stress will induce strain and the area under the stress-strain curve is used to calculate the amount of energy being input into the material. In perfect elastic materials, all the energy going into the material is recovered during unloading. In contrast, for viscoelastic material, not all the applied energy can be recovered; therefore, in this case a retained part of the energy is related to mechanical fatigue of the material and can therefore be interpreted as dissipated energy.

In this regard, Van Dijk (1975) proposed an approach related to the dissipated energy to characterise the fatigue performance of asphalt mixture. Generally, in the fatigue process two stages are distinguished: initiation of micro-cracks and propagation of micro and macro-cracks leading to specimen and material failure. In both stages some energy is dissipated during a single load cycle and can be calculated as explained in Equation (1):

$$W_n = \pi \cdot \sigma_n \cdot \varepsilon_n \cdot \sin\theta_n \quad (1)$$

Where: n = number of load cycle; ε = strain amplitude; σ = stress amplitude; θ = phase angle.

Based on this concept and Van Dijk's work, Hopman et al. (1989) proposed the use of an energy ratio to define the number of cycles (N_{f1}) in a controlled strain mode to a point where cracks are considered to initiate, which is calculated as Equation (2):

$$R_i = \frac{n.w_0}{} \quad (2)$$

Where n = number of load cycles, w_0 = dissipated energy at the first cycle and w_i = dissipated energy at the i^{th} cycle. However, in 1993, Rowe simplified the equation proposed by Hopman to identify the number of cycles (N_{f1}) when cracks are conceded to initiate and, more accurately, it is a point where the micro-cracks coalesce to form a sharp crack (Rowe, 1993; Rowe and Bouldin, 2000).

In controlled strain mode, the equation of energy ratio can be written as following:

$$R_i^{\varepsilon} = \frac{n}{G_i^*} \quad (3)$$

Where R_i^{ε} is energy ratio at controlled strain mode and G_i^* is the complex shear modulus at the i^{th} cycle.

N_{f1} can be defined in this mode as the point at which the slope of the dissipated energy ratio as a function of load cycles diverts from a straight line; whereas, for the controlled stress mode, N_{f1} corresponds to the peak value when the energy ratio is plotted against number of load cycle and the simplified equation of calculation energy ratio as:

$$R_i^{\sigma} = n.\,E_i^* \quad (4)$$

Where E_i^* is the energy ratio at controlled stress mode.

The results of this approach are shown in Table 7. It can be noticed from Table 3 and Figure 4 that:

1. Increase IFLR parameter with increase the proportion of micro silica added to the extent of 2% and then decreases with increasing percentage of micro silica,
2. The IFLR increased when the percentage of GG increased in the strain mode and reduced in the stress mode,
3. The ILFR parameter increased with increased percentage of SBS1101 additives until 3% and then reduced,
4. Adding 6% of SBS1184 significantly improved the fatigue life of bitumen,
5. In strain mode cases, fatigue performance of Nasiriyah asphalt binder is better than Durah and vice versa in stress mode. Examples of the N_{f1} and how it is calculated are provided in Figures A2, 6, 10 and 14 in the Appendix.

Ratio of dissipated energy change (RDEC)

The ratio of dissipated energy change (RDEC) approach was introduced by Carpenter and Jansen (1997). The RDEC approach is perhaps the most refined energy method, which can be used to extrapolate fatigue life. The RDEC is defined as the difference in dissipated energy between two loading cycles which contributes to damage. In other words, the area found inside a hysteresis loop (created during cyclic loading and unloading of asphalt binder) is the dissipated energy. The difference in area of each loop indicates the damage produced by dissipated energy (Shen and Carpenter, 2007). This RDEC can be calculated based on Equation (1). The typical cycle count between a and b for RDEC calculation is 100, that is, b-a=100. Larger numbers such as 1000 or 10000 can be used when the DE change between every 100 cycles is too small to recognise. Such

Table 7. Energy ratio method.

Parameter	Av. Increased Fatigue Life Ratio (IFLR) with standard division (σ)							
	Nasiriyah Asphalt				Durah Asphalt			
	Strain mode		Stress mode		Strain mode		Stress mode	
	$Nf_{50\%}$	σ	$Nf_{10\%}$	σ	$Nf_{50\%}$	σ	$Nf_{10\%}$	σ
2%s	0.783	1.27134783	5.500	1.581 85	1.136	1.861	3.421	1.248
4%s	0.674	1.09477174	0.875	0.864 36	0.864	1.414	1.842	0.672
6%s	0.522	0.84756522	3.938	3.888 63	0.818	1.340	2.895	1.056
6%GG	0.478	0.77693478	0.188	0.185 51	1.364	2.233	1.263	1.724
9%GG	0.565	0.91819565	2.875	2.839	1.273	2.084	0.526	0.718
3%SBS1101	0.674	1.09477174	0.875	0.864	0.545	1.439	6.053	3.661
6%SBS1101	0.609	1.59752174	1.375	1.351	0.409	1.079	3.684	2.228
9%SBS1101	0.370	0.96992391	2.938	2.903	0.273	0.719	6.184	3.740
3%SBS1184	0.696	1.82573913	1.688	1.635	0.773	2.038	6.579	3.979
6%SBS1184	0.935	2.45333696	1.781	1.751	0.727	1.918	2.368	1.432
9%SBS1184	0.739	1.93984783	1.125	1.104	0.477	1.259	1.842	1.114

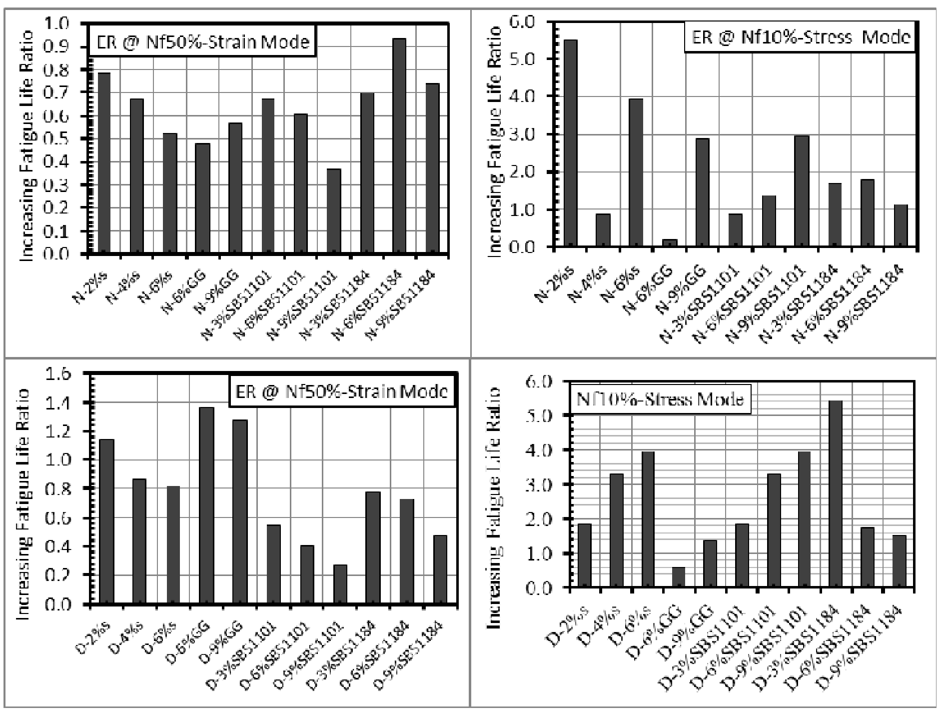

Figure 4. IFLR for the energy ratio method approach.

definition of RDEC provides a true indication of the damage being done to the mixture from one cycle to another by comparing the previous cycle's energy level and determining how much of it contributed to the damage (Shen and Carpenter, 2007):

$$RDEC_a = \frac{DE_a - DE_b}{DE_a * (b-a)} \quad (5)$$

where: a and b = loading cycle at points a and b, respectively; $RDEC_a$ = the average ratio of dissipated energy change at cycle a, compare to cycle b; and DE_a and DE_b = dissipated energy at cycle a and b, respectively, which were calculated directly by fatigue testing.

Previous studies by Ghuzlan (2001) and Carpenter et al. (2003) described the damage curve using the RDEC versus loading cycles shown in Figure 5. It can be seen

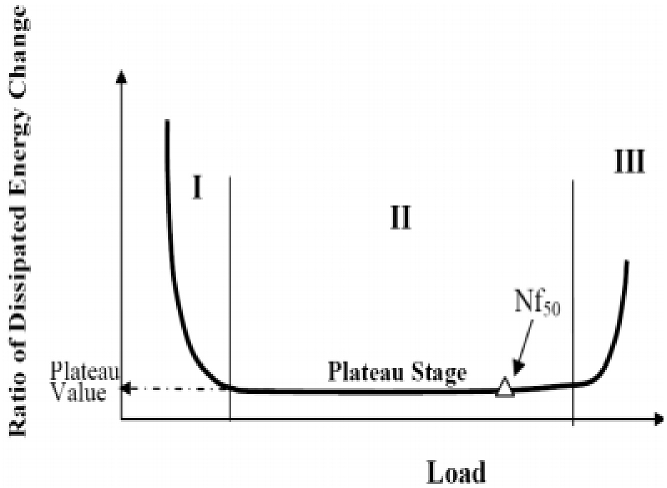

Figure 5. Plateau value calculation (Carpenter et al., 2003).

that the damage curve is separated into three stages: The initial period (Stage I), the plateau period (Stage II), and the failure period (Stage III). Stage I shows a rapidly decreasing dissipated energy ratio which indicates 'settling' of sample. The average dissipated energy ratio in Stage II is known as plateau value. The plateau stage is when a constant percentage of dissipated energy produces damage. This behavior continues until an increase in dissipated energy ratio occurs which signifies fatigue failure and unstable crack propagation (Stage III). From the plateau stage (Stage II), a value can be determined which indicates fatigue failure in a sample. This is called the Plateau Value and is defined as the RDEC value at the number of cycles equal to the failure point ($N_{f=50\%}$). Failure is defined as a 50% reduction in initial stiffness, with the initial stiffness being determined at the 50th loading cycle. Lower PVs correspond to longer fatigue lives (Ghuzlan and Carpenter, 2000). According to Carpenter and Shen (2005, 2006, 2009), the PV-$N_{f=50\%}$ relationship is not mixture-specific and is supposedly independent of temperature, mode of loading, frequency, and healing capacity (rest periods). Ghuzlan and Carpenter (2000) showed that the plateau value relates precisely to the true fatigue failure (Stage III).

They also proposed a simplified RDEC approach where the dissipated energy must be fitted by a power law relationship with the number of load cycles to obtain the slope (b) of the model as follows:

$$PV = a\,(N_{f50})^{b} \tag{6}$$

The slopes (b) of power law model and plateau value were calculated and are presented in Table 8 and Figure 6. The analysis of Figure 6 allows us to state that the plateau value calculated can be used to predict the fatigue life of asphalt binder.

From Table 5, the $N_{f\ (50\ or\ 10\%)}$ to starting Stage III (failure point) can be seen for different cases:

1. Adding 2 to 4% silica reduced the PV and so that increased the required cycle number to propagate the crack,
2. The PV reduced when percentage of GG increased,
3. Adding SBS1184 reduced the PV and increased the ability of the asphalt binder to resist fatigue,
4. In strain mode cases, fatigue performance of Nasiriyah asphalt binder is better than Durah asphalt binder.

Energy stiffness ratio (ESR)

By applying Abojaradeh's method (Abojaradeh et al., 2007), a new rational fatigue failure criterion was developed based on the Rowe and Bouldin failure definition (Rowe and Bouldin, 2000) by normalising the Rowe and Bouldin energy ratio ($N_i{*}S_i$) by dividing it by the initial stiffness (S_o), as follows:

$$ESR = \frac{N_i * S_i}{S_o} \tag{7}$$

where ESR is energy stiffness ratio, N_i is the cycle number, S_i is the stiffness at i^{th} cycle and S_o is the initial stiffness taken at cycle number 50. In this study, using complex shear modulus and plotting the energy stiffness ratio value ($N_i{*}G_i/G_o$) versus the number of loading cycles, a peak value can be obtained, as shown in the example in Figures A3, 7, 11 and 15 in the Appendix.

The reason that the energy stiffness ratio increases before it reaches its peak is that the value of N_i continuously increases during the test, whereas the G_o value is constant. The value of G_i during this time might be lightly decreasing. After reaching its peak, the energy stiffness ratio decreases suddenly because of the sudden decrease in the stiffness of the material even with the increase of the N_i value. Thus, failure is defined as the number of load repetitions at the peak value of the curve for either constant strain or constant stress mode, as shown in Figure A3. The ESR value at failure, when plotted versus the corresponding number of cycles at failure for all specimens on a log-log scale, results in a straight line relationship with high coefficients of determination, as shown in Figure 7. The results also show that there is little to no significant difference between separate curves for constant stress and constant strain. Excellent fit was obtained for the two modes of loading separately as well as the two modes combined, as shown in Figure 7. Also, the determination of the number of load cycles to failure was straightforward. The regression equation developed in Figure 8 is tabulated in Table 9 and the IFLR for all cases in Table 10.

It can be seen from Table 10 and Figure 9 that:

Table 8. Average of plateau value with number of load cycle caused to failure.

Parameter	Nasiriyah asphalt				Durah asphalt			
	Strain mode		Stress mode		Strain mode		Stress mode	
	$N_{f50\%}$	PV	$N_{f10\%}$	PV	$N_{f50\%}$	PV	$N_{f10\%}$	PV
Pure	23500	6.00E-06	8000	1.30E-05	8000	7.00E-05	4600	1.80E-04
2%s	29500	8.00E-06	44000	2.00E-06	15000	9.00E-06	8600	2.50E-04
4%s	7000	1.50E-06	7000	1.50E-05	8500	4.00E-05	15200	6.00E-04
6%s	16000	3.00E-06	31500	4.00E-06	12000	2.00E-05	18200	4.00E-04
6%GG	11800	2.00E-06	3000	9.00E-05	6000	6.00E-05	2800	1.00E-04
9%GG	26000	6.00E-06	2000	9.00E-05	7000	7.00E-05	6400	3.00E-04
3%SBS1101	21000	6.00E-06	7000	1.00E-05	10000	2.00E-05	8600	3.00E-04
6%SBS1101	22500	6.00E-06	10500	9.00E-06	12000	3.00E-05	15200	4.00E-04
9%SBS1101	21500	4.50E-06	22000	8.00E-06	8000	7.00E-05	18200	6.00E-04
3%SBS1184	19000	4.50E-06	12000	8.00E-06	19000	1.00E-05	25000	8.00E-04
6%SBS1184	32500	5.00E-06	12500	7.00E-06	5000	8.00E-05	8000	4.00E-04
9%SBS1184	26500	4.80E-06	8000	3.00E-05	9000	5.00E-05	7000	3.00E-04

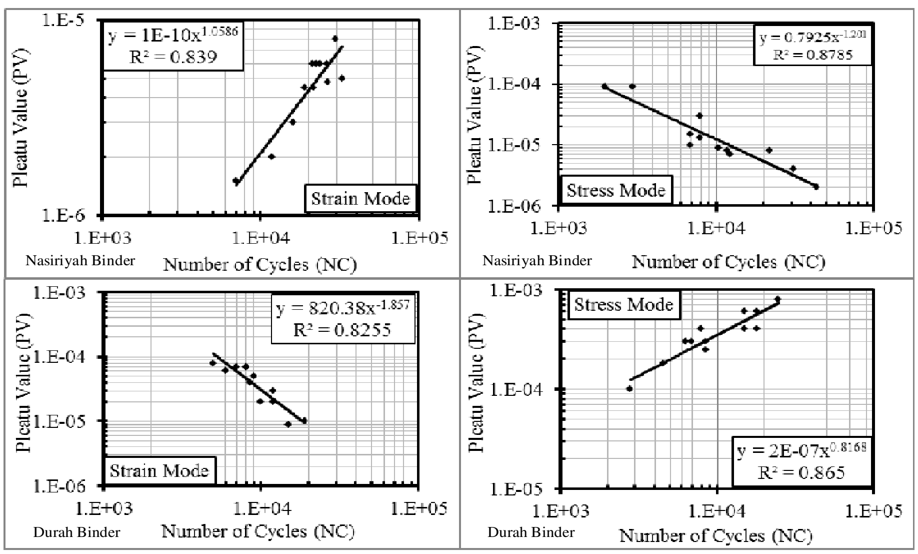

Figure 6. Result of RDEC and calculated plateau value.

1. Adding 2% silica increased fatigue life for the asphalt binder.
2. Increased percentage of GG enhanced the ability of the asphalt binder to resist fatigue.
3. Adding 6% SBS 1184 increased fatigue performance in comparison to SBS 1101.
4. The fatigue performance of Durah asphalt binder is better than that of Nasiriyah asphalt binder.

Viscoelastic continuum damage approach (pseudo-strain approach)

In order to be able to accurately predict the fatigue performance of asphalt binder, advanced mathematical model such as viscoelastic continuum damage (VECD) offers great potential for better understanding of fatigue behavior (Kutay et al., 2008b; Kutay et al., 2008a) and also for modelling the fatigue behavior of modified bitumen.

Kim (2008) successfully applied the elastic-viscoelastic correspondence principle for modelling sand-asphalt mixture behavior under multi-level cyclic loading. With the elastic-viscoelastic correspondence principle, the physical strain (ε) in the elastic theory is replaced with a pseudo-strain, (ε^R). A pseudo-strain is similar to a physical strain, except that it is independent of time or loading history. The pseudo-strain accounts for the linear

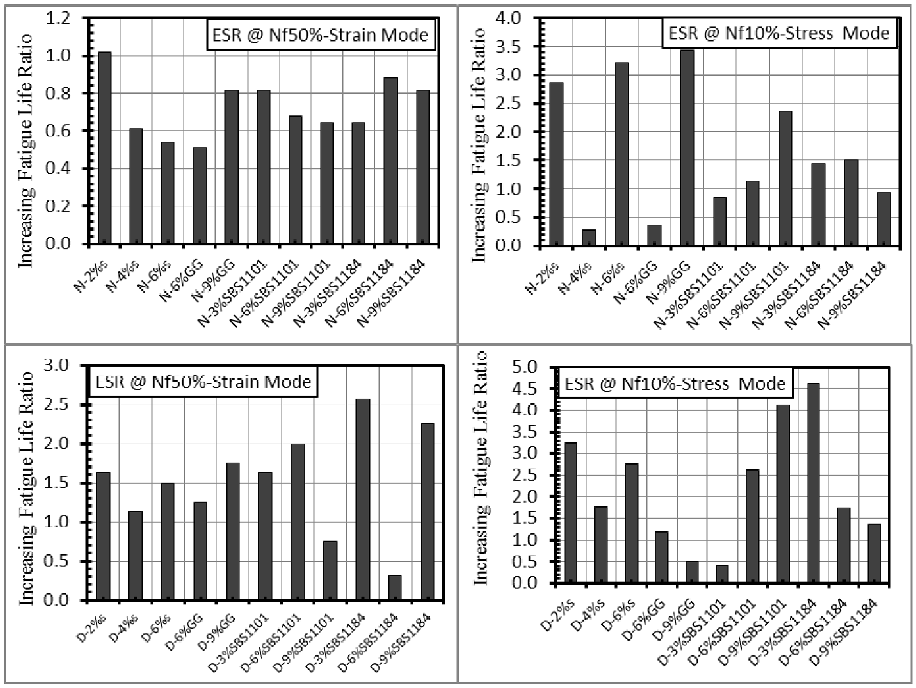

Figure 7. Results of ESR approach.

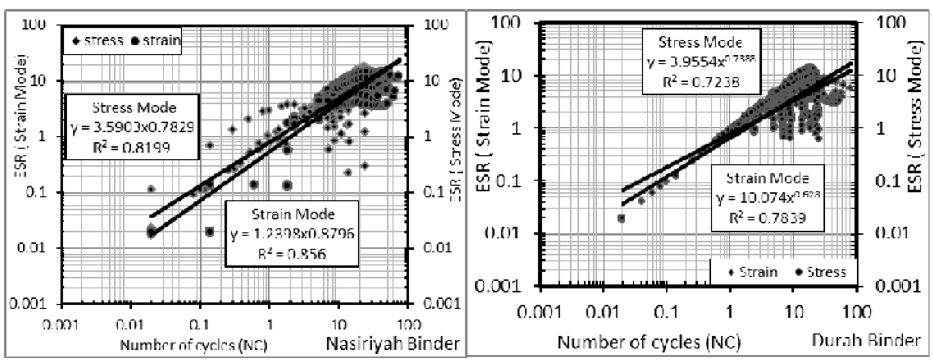

Figure 8. Regression equation for the ESR approach.

viscoelastic hereditary effects of the material through the convolution integral. Thus, damage may be evaluated separately from viscoelastic effects. Without this substitution, identifying damage during cyclic loading is very difficult as there may only be a slight difference in hysteresis loops.

VECD has been successfully used by a number of researchers (Kutay et al., 2008b; Kutay et al., 2008a; Kim and Little, 1990; Kim et al., 1995; Daniel, 2001; Lundstrom and Isacsson, 2003; Christensen Jr and Bonaquist, 2005). Therefore, it would be great to use this approach to rank the performance of modified bitumen. Fatigue can be identified based on the curve of C-S. The (C) parameter is pseudo-stiffness, which is defined as the loss of material stiffness due to loss of material integrity caused by damage, while (S) is a single parameter which is used to quantify the damage growth(Kutay et al., 2008a).

Damage parameter (*S*) is calculated as:

$$S_\varepsilon^{N+\Delta N} = S_\varepsilon^N + \left(\Delta N/f\right)^{\frac{1}{1+\alpha}}\left[-0.5 I \varepsilon_N^{R^2}\left(C_{N+\Delta N} - C_N\right)\right]^{\frac{\alpha}{1+\alpha}} \quad (8)$$

$$S_\sigma^{N+\Delta N} = S_\sigma^N + \left(\Delta N/f\right)^{\frac{1}{1+\alpha}}\left[0.5\frac{1}{I}\sigma_N^{R^2}\left(\frac{1}{C_{N-\Delta N}} - \frac{1}{C_N}\right)\right]^{\frac{\alpha}{1+\alpha}} \quad (9)$$

Where (ε^R) is pseudo-strain, (σ^R) is pseudo-stress, *I* is initial stiffness parameter, C is pseudo-stiffness, *f* is a

Table 9. Regression equation for ESR approach.

Parameter	Nasiriyah Asphalt		Durah Asphalt	
	Predicted equation	R^2	Predicted equation	R^2
Strain	$ESR = 1.2398(NC)^{0.8796}$	0.8560	$ESR = 10.074(NC)^{0.628}$	0.784
Stress	$ESR = 3.5903(NC)^{0.7829}$	0.820	$ESR = 3.9554(NC)^{0.7388}$	0.724

Table 10. Results for ESR approach for all cases.

Parameter	Av. Increased fatigue life ratio (IFLR) and standard division (σ)							
	Nasiriyah Asphalt				Durah Asphalt			
	Strain mode		Stress mode		Strain mode		Stress mode	
	$Nf_{50\%}$	σ	$Nf_{10\%}$	σ	$Nf_{50\%}$	σ	$Nf_{10\%}$	σ
2%s	1.017	3.252	2.857	3.330	1.625	1.271	3.250	2.122
4%s	0.610	2.252	0.286	3.195	1.125	0.763	1.775	0.212
6%s	0.542	1.502	3.214	2.051	1.500	0.678	2.750	2.174
6%GG	0.508	1.252	0.357	2.160	1.250	0.636	1.200	0.353
9%GG	0.814	1.752	3.429	0.900	1.750	1.017	0.500	3.186
3%SBS1101	0.814	1.627	0.857	0.765	1.625	1.017	0.425	0.646
6%SBS1101	0.678	2.628	1.143	2.726	2.000	0.848	2.625	1.129
9%SBS1101	0.644	0.986	2.357	1.227	0.750	0.805	4.125	3.128
3%SBS1184	0.644	3.367	1.429	3.739	2.563	0.805	4.625	1.911
6%SBS1184	0.881	0.625	1.500	1.793	0.313	1.102	1.750	2.481
9%SBS1184	0.814	4.053	0.929	1.409	2.250	1.017	1.375	1.917

constant frequency, (S_{ε}) is the damage parameter when (ε^{R}) is used in the analysis (strain mode), (S_{σ}) is the damage parameter when (σ^{R}) is used (stress mode), *N* is number of cycles, and α is a material constant related to the rate of damage.

α is calculated based on undamaged rheological properties using the slope of relaxation modulus (Hintz et al., 2011a, b). Lee and Kim suggested that $(\alpha = 1 + {}^{1}/_{m})$ is more suitable for strain controlled tests, whereas $(\alpha = {}^{1}/_{m})$ is suitable for stress mode tests (Kutay et al., 2008a; Lee and Kim, 1998).

m is the maximum slope of the relaxation modulus plotted against time in a log-log scale. In this study, it was difficult to run a relaxation test; therefore, it was decided to use a method developed by Scharpery and Park (1999) to convert sweep frequency test data to the relaxation data, as can be seen in Figure 9:

Where G* is the complex shear modulus and *G*(t)* is the relaxation modulus. The sweep frequency (for each control and modified bitumen) was conducted within the LVER at 25°C.

As previously noted, data were analysed based on the stress mode because, according to VECD theory, a single damage characteristic curve (*C-S*) should exist independently of loading frequency, temperature and mode of loading and (C-S) curves calculated at different temperatures, and at different loading modes should collapse on a single curve (Kutay et al., 2008a).

The main advantages of the VECD approach is that it is based on a constitutive model and the characteristic curve can be utilised to model the behavior of the material under any load history and temperature can be assessed (Kutay et al., 2008a; Kutay et al., 2008b; Daniel, 2001).

Once the damage characteristics of C-S curves were obtained, an exponential best-fit line was fitted to the curves, as in the following equation:

$$C = \exp\left(aS^{b}\right) \qquad (10)$$

Where (a and b) are constant parameters defining the best fit. Those parameters with other equations (Kutay et al., 2008a) could be used to predicate the response of the material to a given loading history. The characteristic curves of Figures A4, 8, 12 and 16 in the Appendix, and Tables 11 and 12 describe how the internal damage changes with additive types and content. The internal damage parameter can be used to represent the degradation of the bitumen. All additive types increased the complex shear modulus of bitumen and also delayed the deterioration (development of micro-cracks) and

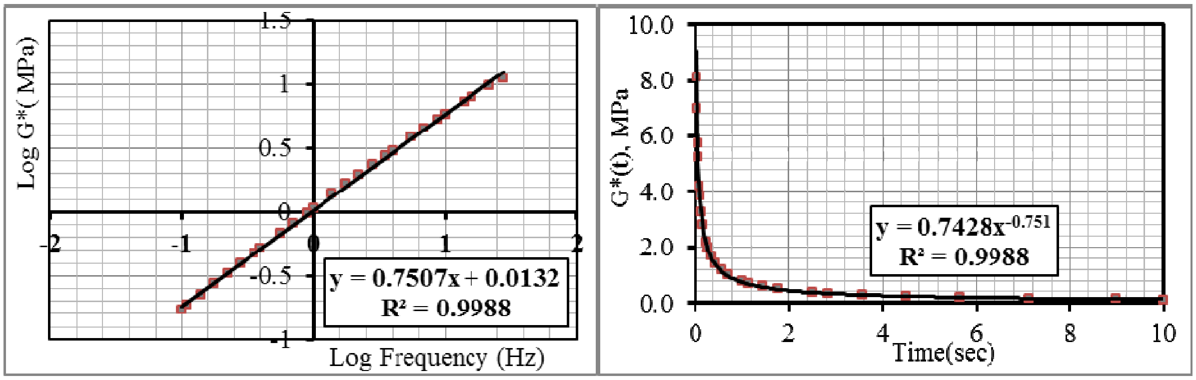

Figure 9. An example of conversion of the sweep frequency data to relaxation data (a) Sweep frequency data (b) Relaxation data.

Table 11. Exponential fit coefficient and *a* parameter of damage characteristics curves of modified bitumen.

Parameter	Strain mode				Stress mode			
	S at C $_{50\%}$	***a***	***b***	**R^2**	**S at C $_{10\%}$**	***a***	***b***	**R^2**
Nasiriyah asphalt binder								
Pure	120	1.1632	-0.008	0.9538	460	1.6838	-0.012	0.8395
2%s	305	1.1136	-0.003	0.9642	515	1.2532	-0.004	0.7605
4%s	110	1.0698	-0.008	0.9895	240	1.5458	-0.018	0.6394
6%s	380	0.9751	-0.002	0.9984	315	1.2031	-0.007	0.9673
6%GG	160	1.1496	-0.005	0.9714	240	1.6188	-0.017	0.8286
9%GG	480	1.0045	-0.002	0.994	660	1.8355	-0.006	0.7661
3%SBS1101	270	1.1748	-0.004	0.9647	340	1.8242	-0.011	0.8677
6%SBS1101	240	1.1026	-0.004	0.9726	480	1.9819	-0.009	0.8036
9%SBS1101	340	1.2168	-0.005	0.9065	680	1.5766	-0.005	0.8986
3%SBS1184	145	1.1320	-0.007	0.9667	510	1.9539	-0.009	0.8562
6%SBS1185	275	1.1035	-0.004	0.9581	480	1.6479	-0.007	0.8903
9%SBS1186	325	1.0608	-0.003	0.9887	380	1.999	-0.01	0.872
Durah asphalt binder								
Pure	200	1.4309	-0.006	0.9771	380	1.7761	-0.01	0.8916
2%s	175	1.5431	-0.008	0.955	600	2.2455	-0.007	0.8892
4%s	225	1.3953	-0.005	0.9763	300	3.6239	-0.013	0.9333
6%s	235	1.4649	-0.004	0.9764	580	2.3507	-0.007	0.8842
6%GG	110	1.3737	-0.01	0.9625	340	3.2109	-0.0015	0.9098
9%GG	120	1.3708	-0.009	0.9783	285	2.2658	-0.017	0.9246
3%SBS1101	205	1.6715	-0.006	0.9562	640	2.1761	-0.006	0.8895
6%SBS1101	215	1.3377	-0.005	0.9683	460	2.8246	-0.008	0.8836
9%SBS1101	260	1.359	-0.004	0.9782	390	2.468	-0.01	0.6098
3%SBS1184	165	1.4565	-0.007	0.9782	640	3.2566	-0.007	0.8873
6%SBS1185	110	1.2638	-0.009	0.9804	480	2.4656	-0.009	0.895
9%SBS1186	180	1.1551	-0.005	0.9808	400	2.1863	-0.009	0.8945

reduced internal damage. Therefore, the performance of this additive should further increase the performance of asphalt binder in terms of fatigue life.

It can be noticed that:

1. Micro silica significantly slowed degradation (internal damage),
2. Adding 6% GG increased the ability of the asphalt binder to resist fatigue and reduced internal damage,

Table 12. Internal damage parameter at 50% stiffness reduction.

Parameter	Av. Internal damage parameter (SP) with standard division (σ)							
	Nasiriyah Asphalt				Durah Asphalt			
	Strain mode		Stress mode		Strain mode		Stress mode	
	$C_{50\%}$	σ	$C_{10\%}$	σ	$C_{50\%}$	σ	$C_{10\%}$	σ
2%s	2.542	1.374	1.120	2.684	0.875	2.871	1.579	4.045
4%s	0.917	1.320	0.522	3.311	1.125	3.096	0.789	3.629
6%s	3.167	1.203	0.685	2.577	1.175	2.800	1.526	2.354
6%GG	1.333	2.223	0.522	3.467	0.550	2.939	0.895	3.215
9%GG	4.000	1.943	1.435	3.932	0.600	3.948	0.750	2.032
3%SBS1101	2.250	2.272	0.739	3.907	1.025	3.940	1.684	1.952
6%SBS1101	2.000	2.463	1.043	2.263	1.075	4.804	1.211	2.534
9%SBS1101	2.833	2.718	1.478	1.800	1.300	3.845	1.026	4.230
3%SBS1184	1.208	2.529	1.109	2.231	0.825	1.367	1.684	3.302
6%SBS1184	2.292	1.362	1.043	1.882	0.550	1.465	1.263	4.226
9%SBS1184	2.708	1.309	0.826	2.283	0.900	1.272	1.053	3.747

3. Adding SBS1184 is better than SBS 1101 to decrease the internal damage in increased fatigue life of the asphalt binder,
4. The fatigue performance of Durah asphalt binder is better than Nasiriyah.

Summary

The above discussion has provided a review of a number of energy-based fatigue failure criteria which have been used by different researchers to assess the fatigue behavior of asphalt binders or mixtures. These criteria appear to be successful under different conditions. However, these criteria usually refer to different stages of failure, crack initiation, propagation, or catastrophic failure. Selecting any one of the failure definitions without fully understanding what stage the failure criteria are referring to can be misleading for the pavement design. The total results are explained in Figure 10.

Conclusions

This paper has presented a comprehensive review of four dissipated energy-based fatigue failure criteria and compared them with the traditional 50 and 20% initial modulus deduction failure criteria (N_{f50} and N_{f20}). Fatigue-testing data for asphalt binders under strain-controlled and stress-controlled conditions were analysed using different approaches. Based on the review and evaluation, the following findings and conclusions are drawn the fatigue data used in this paper are mainly based on DSR testing for binders:

1. The energy ratio approach provides a means by which to determine the number of cycles to crack initiation, N_1. It can be used for asphalt binders under strain-controlled and stress-controlled conditions. However, it should be noted that N_1 is hard to determine practically and it generally has a low correlation with other failure criteria,
2. N_{f20} is more suitable for assessing the fatigue performance in a strain-controlled test. It can be used to refer to the start of micro-crack propagation, and corresponds to the beginning of the plateau stage as defined in the RDEC approach,
3. The dissipated energy approach provides comprehensive information on the internal deformation mechanisms of asphalt binder and can be adopted for evaluating the degradation resistance. The dissipated energy approach provides a reliable estimation method for performance ranking of the asphalt binder,
4. The number of cycles to failure determined from VECD and DE approaches are highly correlated there is only a difference in the definition of when the failure occurs,
5. The RDEC principles are very interesting because they focus the attention on the change of DE. The fatigue life based on the RDEC (true failure) approach is longer than the fatigue lives based on the other approach,
6. Adding 2% silica works to improve the efficiency of local asphalt to resist fatigue cracks due to decreasing the proportion of internal damage and increasing viscosity and thus increasing the fatigue life,
7. Whenever a growing proportion of GG over 6% increases the viscosity of the asphalt binder reduced the amount of internal deformation and less than the amount of dissipated energy and thus increasing its ability to resist fatigue cracks,
8. Adding both types of polymer improves the performance of the asphalt binder to resist fatigue cracks but using 6% SBS 1184 is the best way to increase the viscosity of the asphalt and reduce the amount of internal

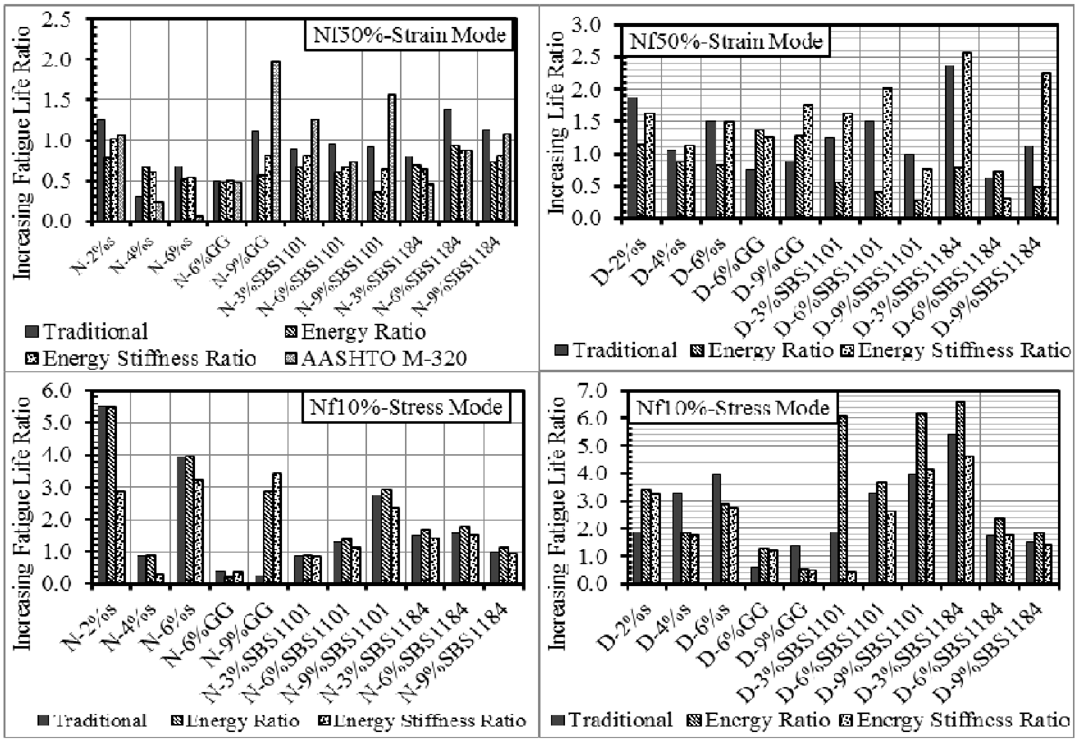

Figure 10. Comparison with different fatigue approaches.

deformation and dissipated energy during each cycles,

7. Performance of the asphalt product from Durah to resist fatigue cracks is better than the asphalt product from the Nasiriyah refinery, so it is advised to use the former in flexible pavements in the middle and southern regions of Iraq with the use of proposed proportions of additives, referred to previously,

8. The fatigue life can be predicted from plateau value. When the plateau values decreased (the dissipated energy per each cycle will be reduced) the number of load cycles required to propagate the crack.

Conflict of Interest

The author has not declared any conflict of interest.

ACKNOWLEDGMENTS

The writer sincerely thanks Dr Hussain A. Khalid at the University of Liverpool for allowing the use of DSR to evaluate the local asphalt binders.

REFERENCES

Abojaradeh M, Witczak MW, Mamlouk MS, Kaloush KE (2007). Validation Of Initial And Failure Stiffness Definitions In Flexure Fatigue Test For Hot Mix Asphalt, J. Test. Eval. 35:95.

Airey G, Thom N, Osman S, Huang H, Collop A, Petit C, Al-Qadi I, Millien A (2004). A Comparison Of Bitumen/Mastic Fatigue Data From Different Test Methods". Fifth International Rilem Conference On Reflective Cracking In Pavements, Rilem Publications Sarl, pp. 383-390.

Anderson DA, Hir YML, Marasteanu MO, Planche J-P, Martin D, Gauthier G (2001). "Evaluation Of Fatigue Criteria For Asphalt Binders". Transportation Research Record: J. Transport. Res. Board. 1766:48-56. http://dx.doi.org/10.3141/1766-07

Artamendi I, Khalid H (2005). Characterization Of Fatigue Damage For Paving Asphaltic Materials, Fatigue. Fract. Eng. Mater. Struct. 28:1113-1118.http://dx.doi.org/10.1111/j.1460-2695.2005.00949.x

Bahia H, Hanson D, Zeng M, Zhai H, Khatri M, Anderson M (2000). A Project Nchrp 9-10 "Superpave Protocols For Modified Asphalt Binders". Draft Topical Report (Task 9), Prepared For National Cooperative Highway Research Program, Transportation Research Board, National Research Council.

Bahia HU, Zhai H, Bonnetti K, Kose S (1999). Non-linear viscoelastic and fatigue properties of asphalt binders. J. Assoc. Asphalt Paving Technol. 68:1-34.

Bahia HU, Zhai H, Zeng M, Hu Y, Turner P (2001). Development Of Binder Specification Parameters Based On Characterization Of Damage Behavior (With Discussion)". J. Assoc. Asphalt Paving Technol. P. 70.

Bonnetti KS, Nam K, Bahia HU (2002). Measuring And Defining Fatigue Behavior Of Asphalt Binders". Transportation Research Record: J. Transport. Res. Board 1810:33-43.

Carpenter SH, Jansen M (1997). Fatigue Behavior Under New Aircraft Loading Conditions". Aircraft/Pavement Technology In The Midst Of Change.

Carpenter SH, Shen S (2005). Application Of The Dissipated Energy Concept In Fatigue Endurance Limit Testing". Transportation Research Record: J. Transport. Res. Board 1929:165-173.

Christensen Jr DW, Bonaquist R (2005). Practical Application Of Continuum Damage Theory To Fatigue Phenomena In Asphalt

Concrete Mixtures (With Discussion And Closure)". J. Assoc. Asphalt Paving Technol, P. 74.
Carpenter SH, Shen S (2006). Dissipated Energy Approach To Study Hot-Mix Asphalt Healing In Fatigue". Transportation Research Record: J. Transport. Res. Board, 1970, pp. 178-185. http://dx.doi.org/10.3141/1970-21
Daniel JS (2001). Development Of A Simplified Fatigue Test And Analysis Procedure Using A Viscoelastic, Continuum Damage Model And Its Implementation To Westrack Mixtures".
Deacon JA, Coplantz JS, Tayebali AA, Monismith CL (1994). Temperature Considerations In Asphalt-Aggregate Mixture Analysis And Design", Transportation Research Record.
Ghuzlan KA (2001). Fatigue Damage Analysis In Asphalt Concrete Mixtures Based Upon Dissipated Energy Concepts", Phd Thesis University Of Illinois At Urbana-Champaign.
Ghuzlan KA, Carpenter SH (2000). Energy-Derived, Damage-Based Failure Criterion For Fatigue Testing". Transportation Research Record: J. Transport. Res. Board, 1723:141-149. http://dx.doi.org/10.3141/1723-18
Ghuzlan KA, Carpenter SH (2006). Fatigue Damage Analysis In Asphalt Concrete Mixtures Using The Dissipated Energy Approach, Canad. J. Civil Eng. 33:890-901. http://dx.doi.org/10.1139/l06-032
Harvey J, Cebon D (2003). Failure Mechanisms In Viscoelastic Films", J. Mater. Sci. 38:1021-1032.
Hintz C, Velasquez R, Johnson C, Bahia H (2011a). Modification And Validation Of Linear Amplitude Sweep Test For Binder Fatigue Specification. Transportation Research Record: J. Transport. Res. Board, 2207:99-106. http://dx.doi.org/10.3141/2207-13
Hintz C, Velasquez R, Johnson C, Bahia H (2011b). Modification And Validation Of Linear Amplitude Sweep Test For Binder Fatigue Specification". Transportation Research Record: J. Transport. Res. Board, 2207:99-106.
Hopman P, Kunst P, Pronk A (1989). A Renewed Interpretation Method For Fatigue Measurements, Verification Of Miner's Rule", 4th Eurobitume Symposium In Madrid, pp. 557-561.
Isacsson U, Lu X (1995). Testing And Appraisal Of Polymer Modified Road Bitumens-State. Art. Mater. Struct. 28:139-159. http://dx.doi.org/10.1007/BF02473221
Khodary MHF (2010). Evaluation Of Fatigue Resistance For Modified Asphalt Concrete Mixtures Based On Dissipated Energy Concept",Phd Thesis, Department Of Civil Engineering And Geodesy Tu Darmstadt.
Kim Y, Lee Y, Lee H (1995). Correspondence Principle For Characterization Of Asphalt Concrete, J. Mater. Civil Eng. 7:59-68. http://dx.doi.org/10.1061/(ASCE)0899-1561(1995)7:1(59)
Kim YR (2008), "Modeling of asphalt concrete", ASCE Press-USA.
Kim YR, Little DN (1990). One-Dimensional Constitutive Modeling Of Asphalt Concrete, J. Eng. Mech. 116:751-772. http://dx.doi.org/10.1061/(ASCE)0733-9399(1990)116:4(751)
Kutay M, Gibson N, Youtcheff J (2008a). Use Of Pseudostress And Pseudostrain Concepts For Characterization Of Asphalt Fatigue Tests", Chapter 30, Pavement Cracking: Mechanisms, Modeling, Detection, Test. Case Histor. pp. 305-314.
Kutay ME, Gibson N, Youtcheff J (2008b). Conventional And Viscoelastic Continuum Damage (Vecd)-Based Fatigue Analysis Of Polymer Modified Asphalt Pavements (With Discussion). J. Assoc. Asphalt Pav. Technol. P. 77.
Lee H-J, Kim YR (1998). Viscoelastic Constitutive Model For Asphalt Concrete Under Cyclic Loading, J. Eng. Mech. 124:32-40. http://dx.doi.org/10.1061/(ASCE)0733-9399(1998)124:1(32).
Lundstrom R, Isacsson U (2003). Asphalt Fatigue Modelling Using Viscoelastic Continuum Damage Theory, Road Mater. Pave. Design 4:51-75. http://dx.doi.org/10.1080/14680629.2003.9689940
Nicholls C (2006). Bitval–Analysis Of Available Data For Validation Of Bitumen Tests". Report On Phase, P. 1.
Phillips MC (1998). Multi-step models for fatigue and healing, and binder properties involved in healing. In Eurobitume workshop on performance related properties for bituminous binders, Luxembourg.
Rowe G (1993). Performance Of Asphalt Mixtures In The Trapezoidal Fatigue Test, Asphalt Pav. Technol. 62:344-344.
Rowe GM, Bouldin MG (2000). Improved Techniques To Evaluate The Fatigue Resistance Of Asphaltic Mixtures". 2nd Eurasphalt and Eurobitume Congress Barcelona,
Shen S, Carpenter SH (2007). Development Of An Asphalt Fatigue Model Based On Energy Principles (With Discussion And Closure), J. Assoc. Asphalt Pav. Technol. P. 76.
Sybilski D, Soenen H, Gajewski M, Chailleux E, Bankowski W (2013). Binder Testing" Advances In Interlaboratory Testing And Evaluation Of Bituminous Materials. Springer. http://dx.doi.org/10.1007/978-94-007-5104-0_2; PMid:24505225 PMCid:PMC3908509
Van Dijk W (1975). Practical Fatigue Characterization Of Bituminous Mixes, J. Assoc. Asphalt Pav. Technol. 44:38-72.
Zhu J, Birgisson B, Kringos N (2014). Polymer Modification Of Bitumen: Advances And Challenges. Eur. Poly. J. 54:18-38. http://dx.doi.org/10.1016/j.eurpolymj.2014.02.005

APPENDIX

Nasiriyah asphalt binder

Control strain mode

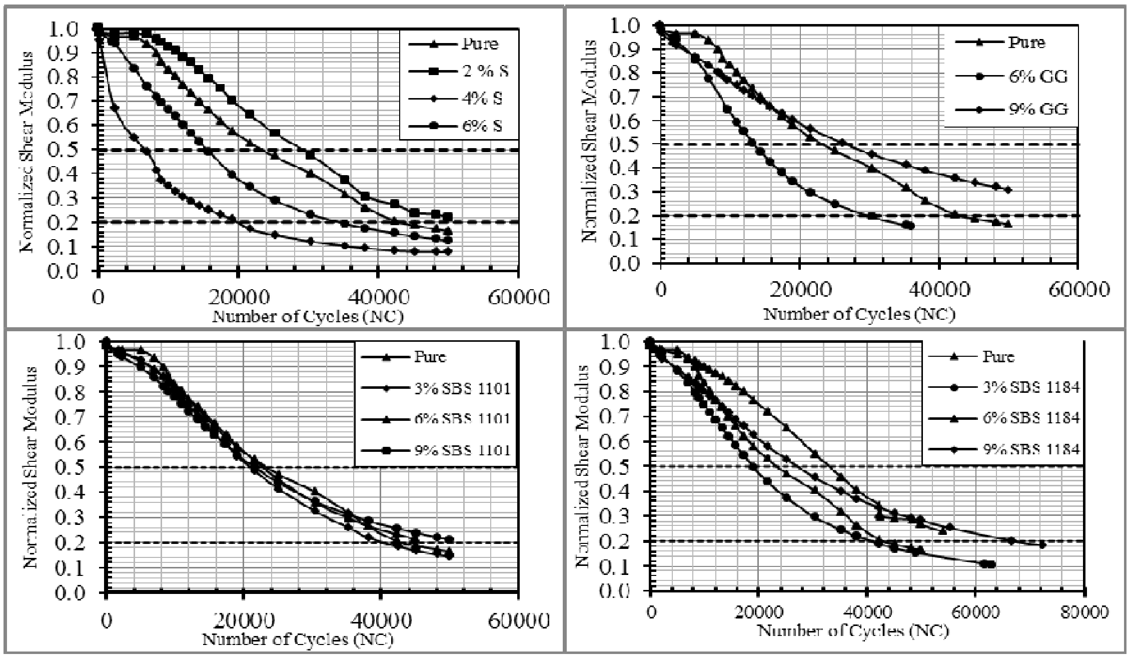

Figure A1. Normalised shear modulus against number of cycles at traditional approach.

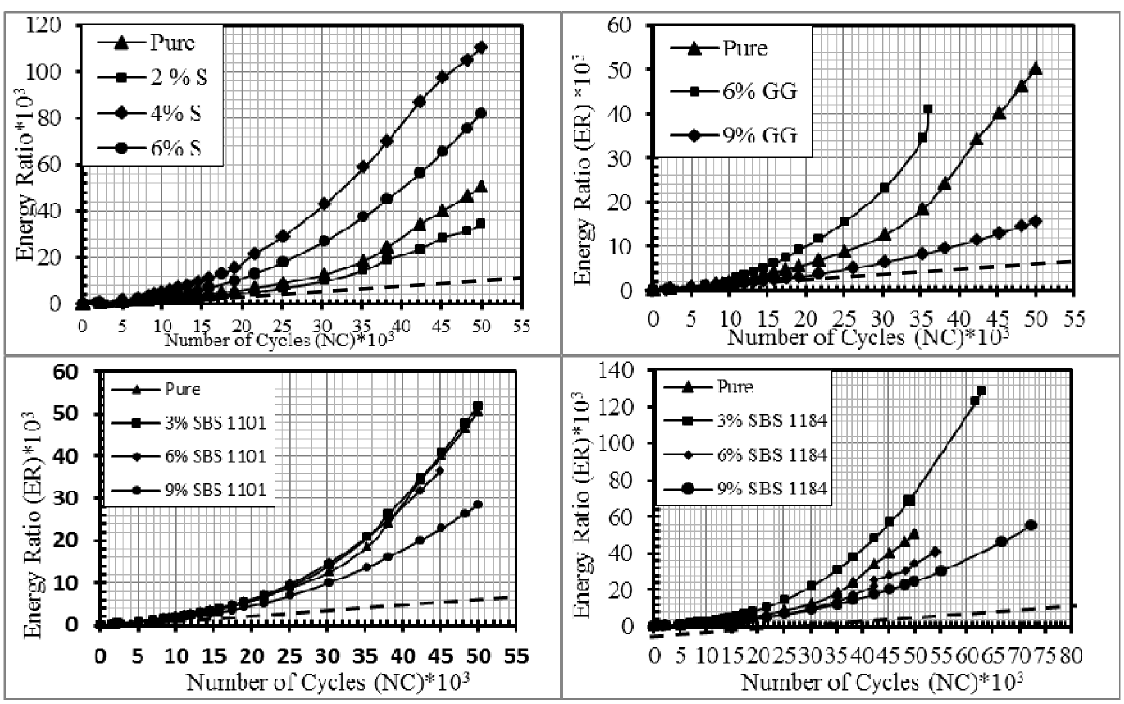

Figure A2. Energy Ratio against number of cycles at energy approach.

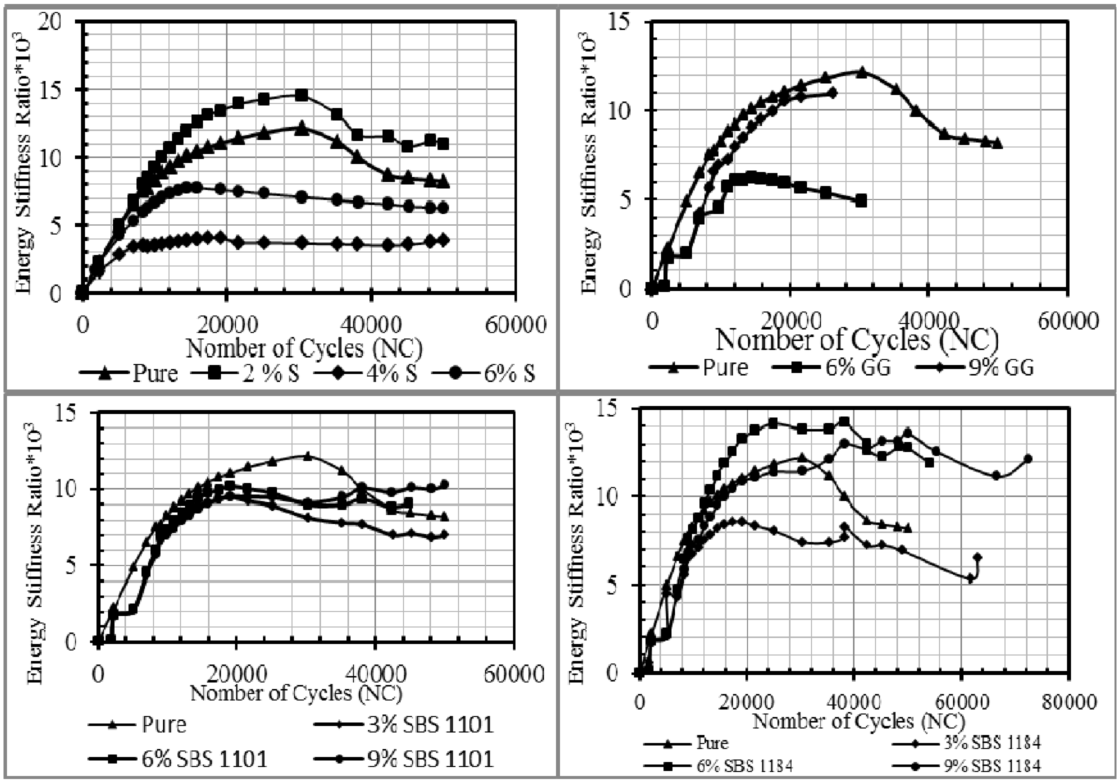

Figure A3. Energy stiffness ratio against number of cycles at energy stiffness approach.

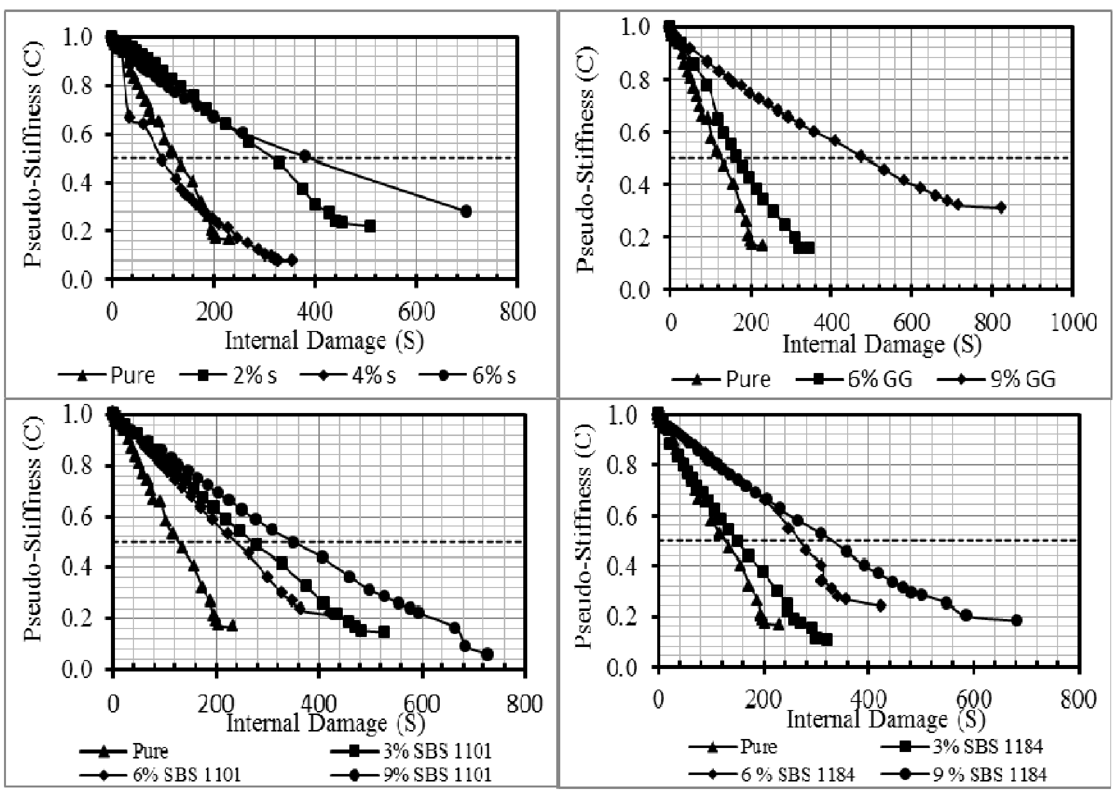

Figure A4. Pseudo-strain-based damage parameter of Nasiriysh asphalt binder.

Control stress mode results

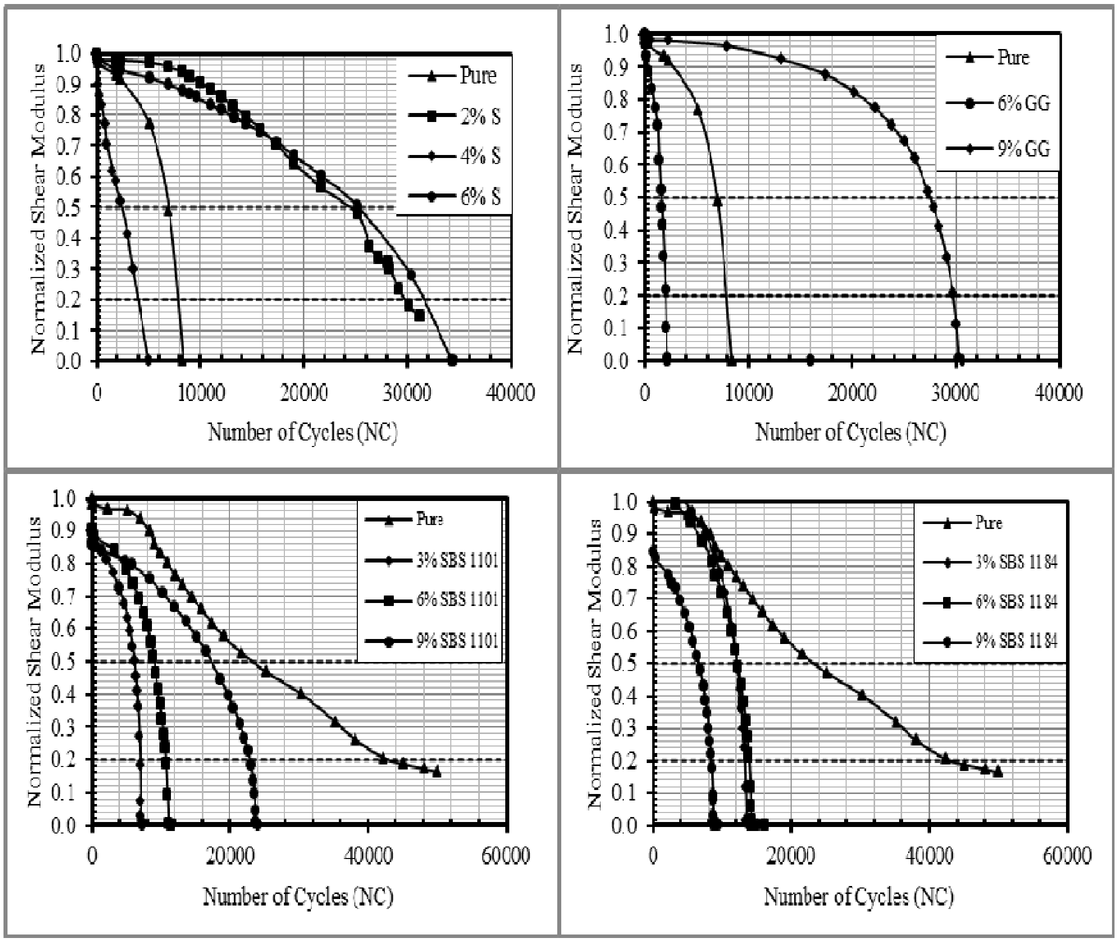

Figure A5. Normalised shear modulus against number of cycles at traditional approach.

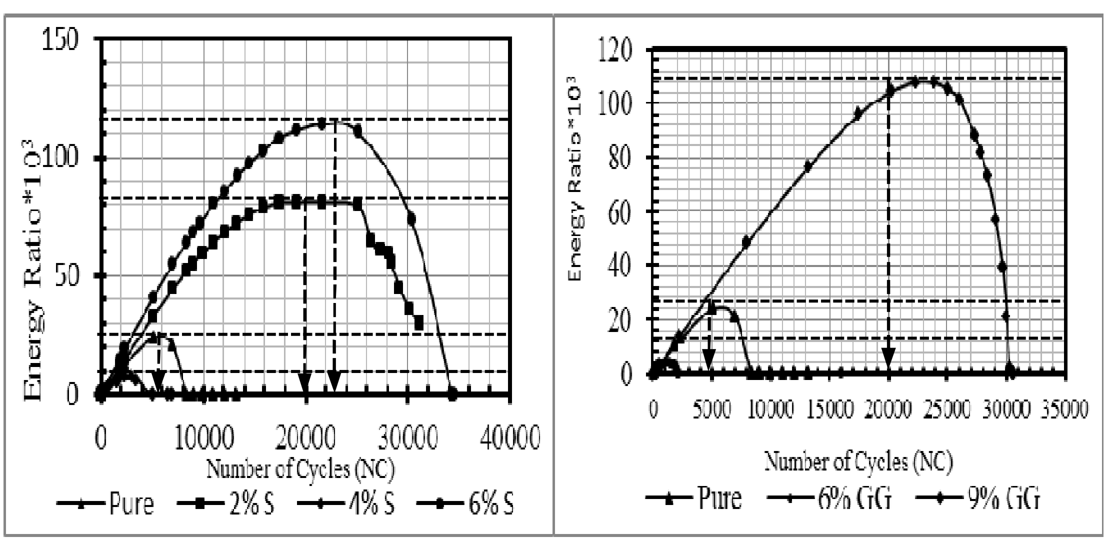

Figure A6. Energy ratio against number of cycles at energy approach.

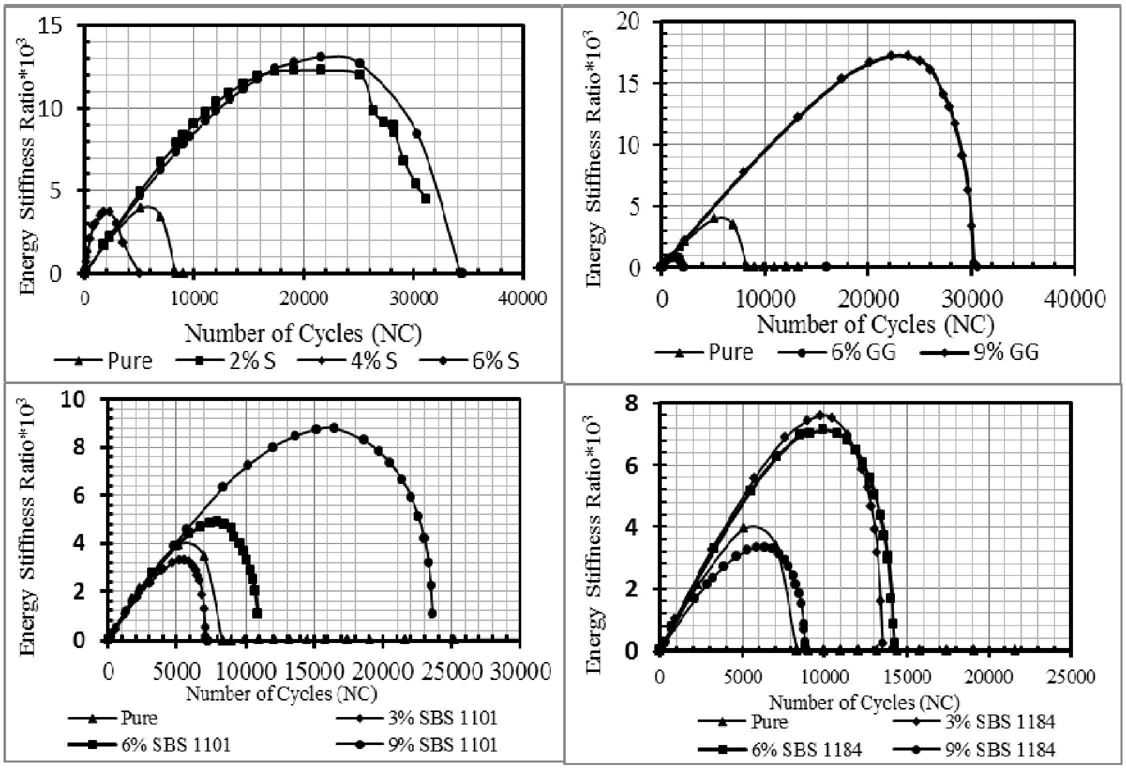

Figure A7. Energy stiffness ratio against number of cycles at energy stiffness approach.

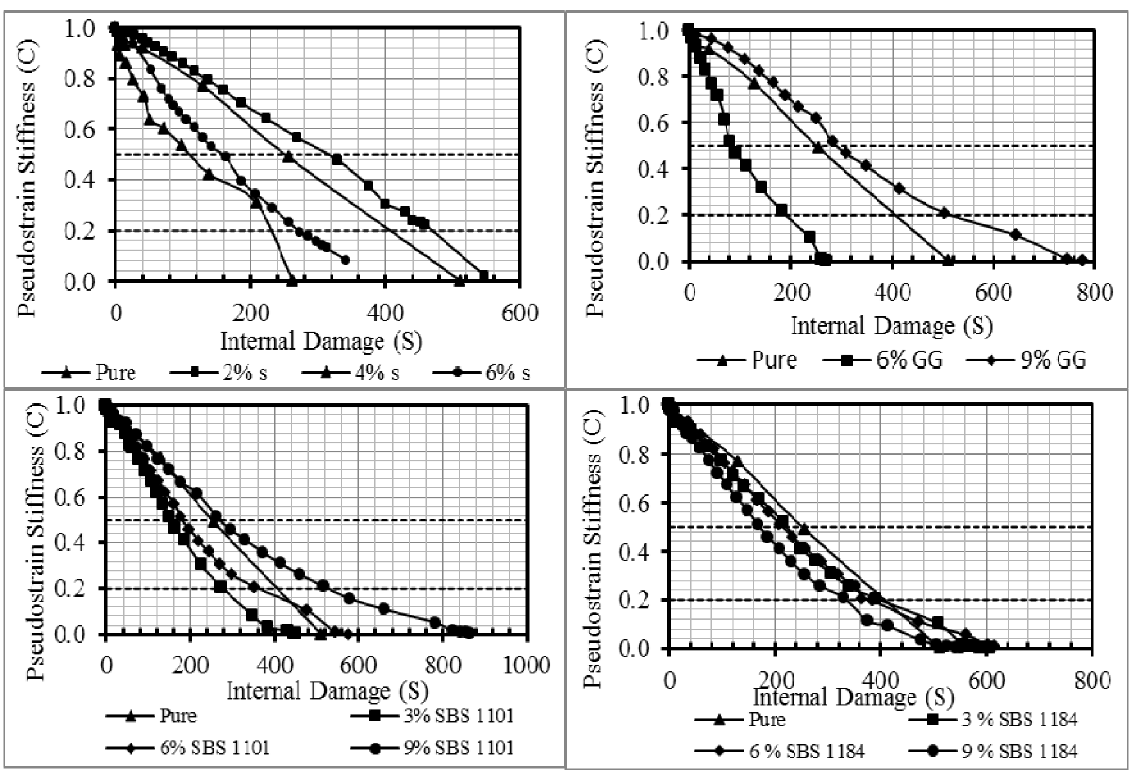

Figure A8. Pseudo-strain-based damage parameter of Nayisirh asphalt binder.

Durah asphalt binder

Control strain mode results

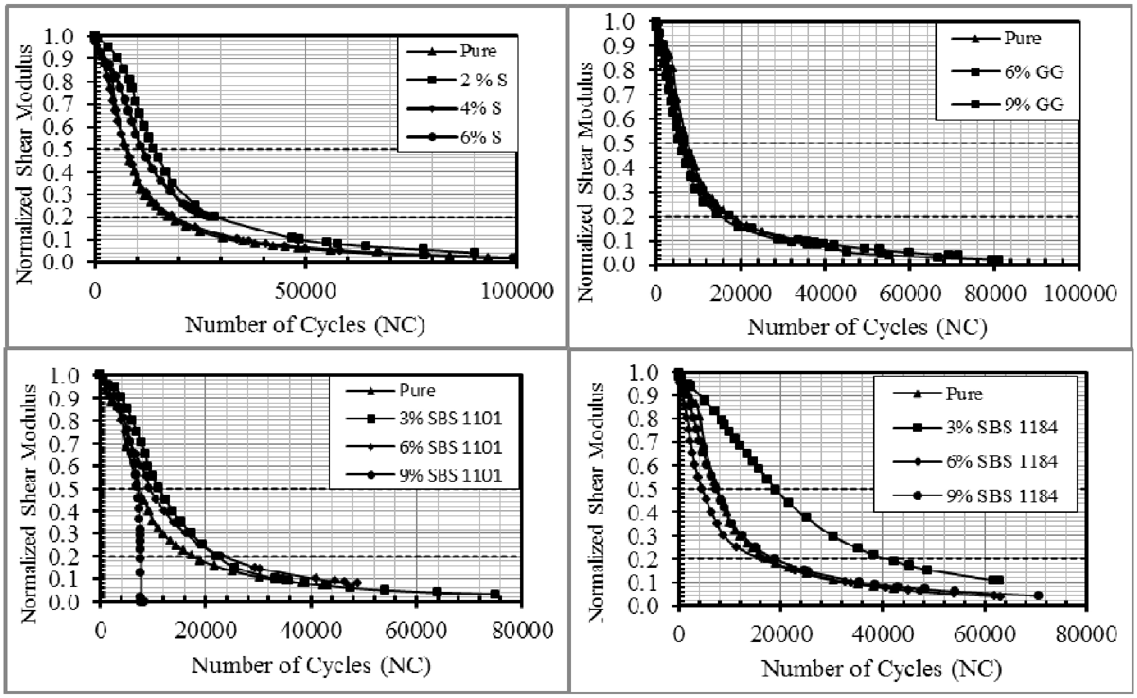

Figure A9. Normalised shear modulus against number of cycles at traditional approach.

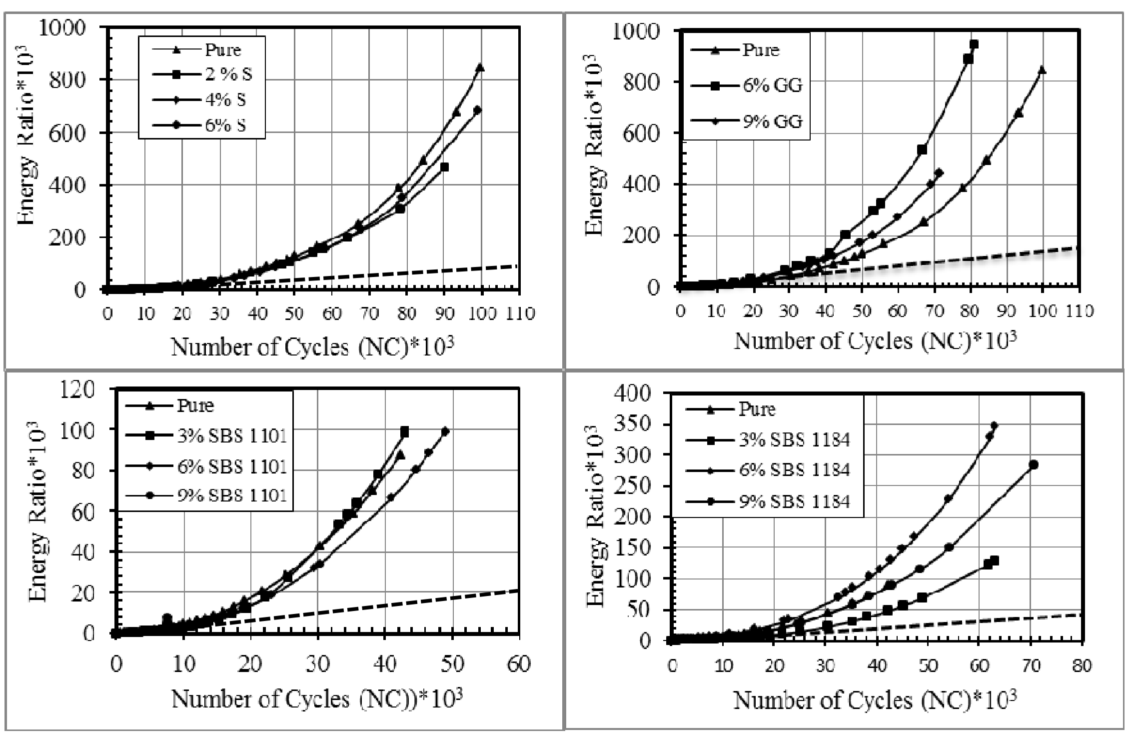

Figure A10. Energy ratio against number of cycles at energy approach.

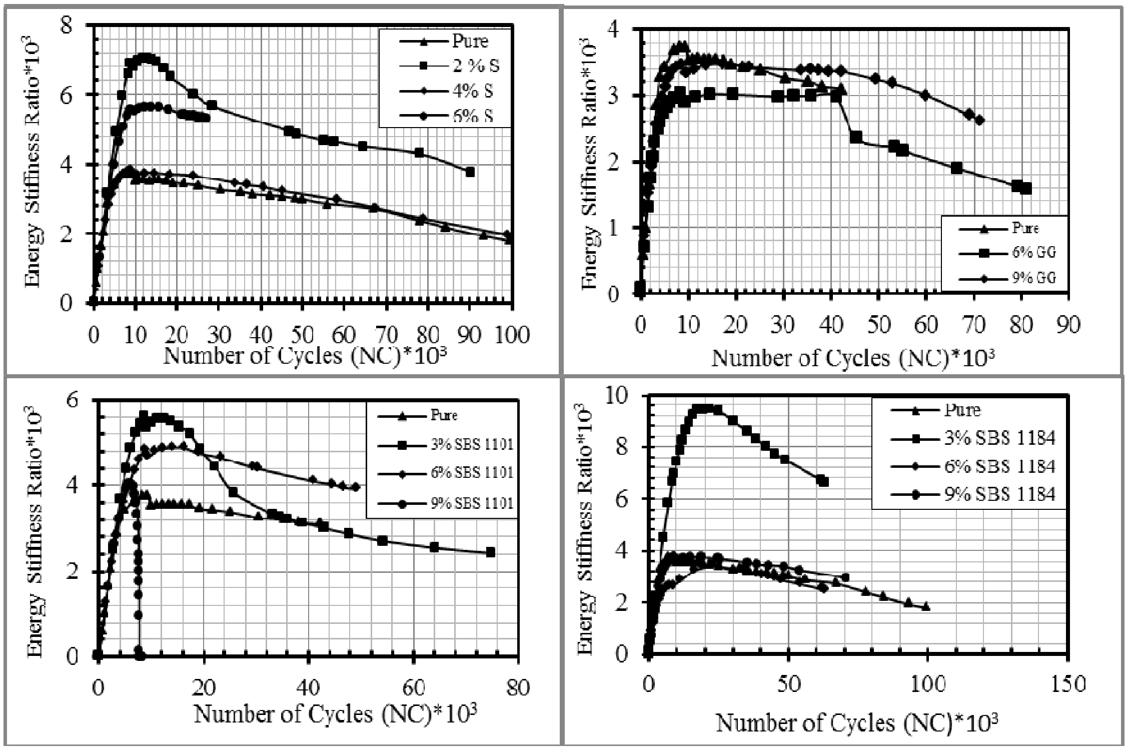

Figure A11. Energy stiffness ratio against number of cycles at energy stiffness approach.

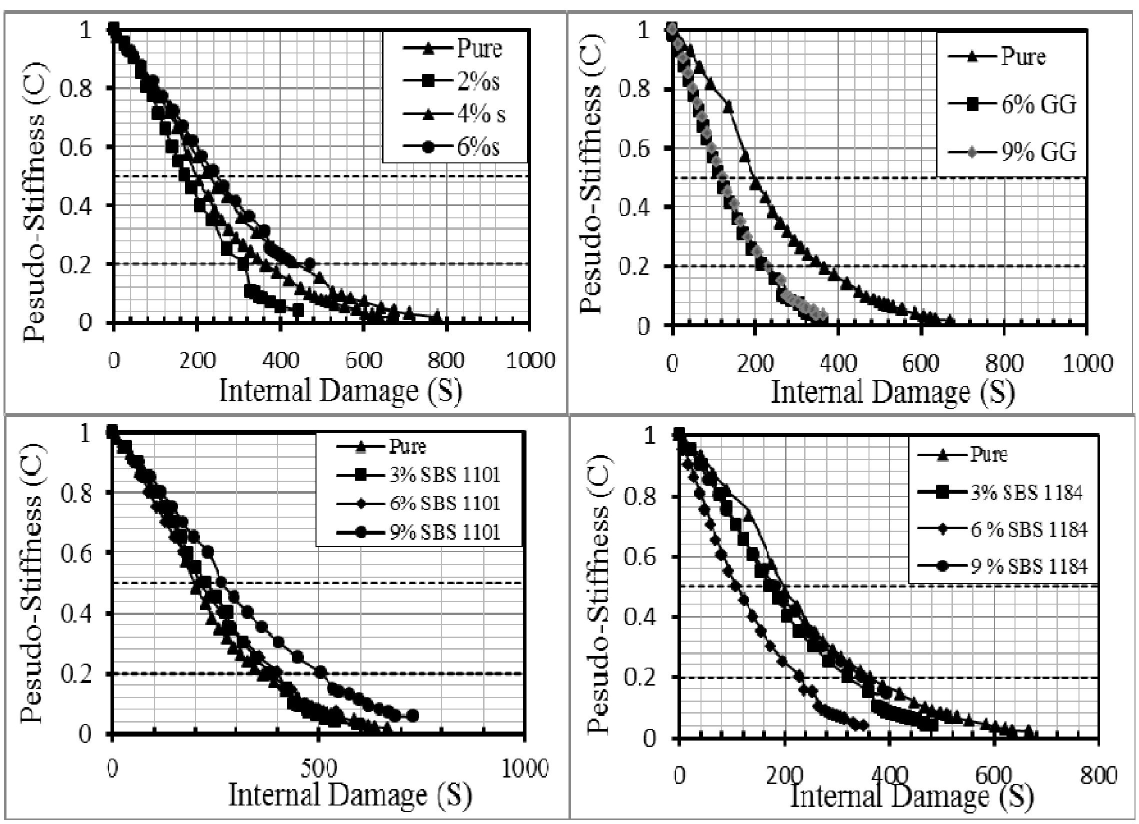

Figure A12. Pseudo-strain-based damage parameter of Durah asphalt binder.

Control stress mode

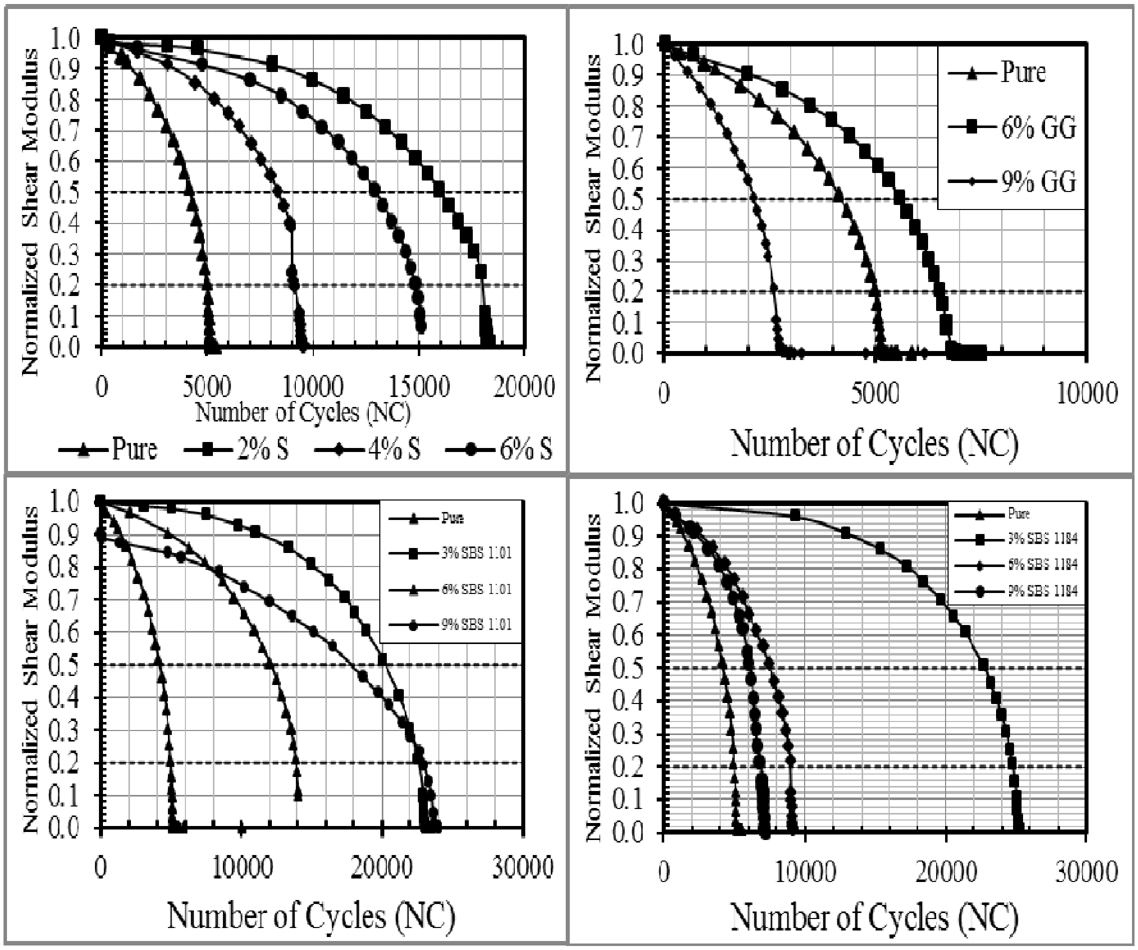

Figure A13. Normalised shear modulus against number of cycles at traditional approach.

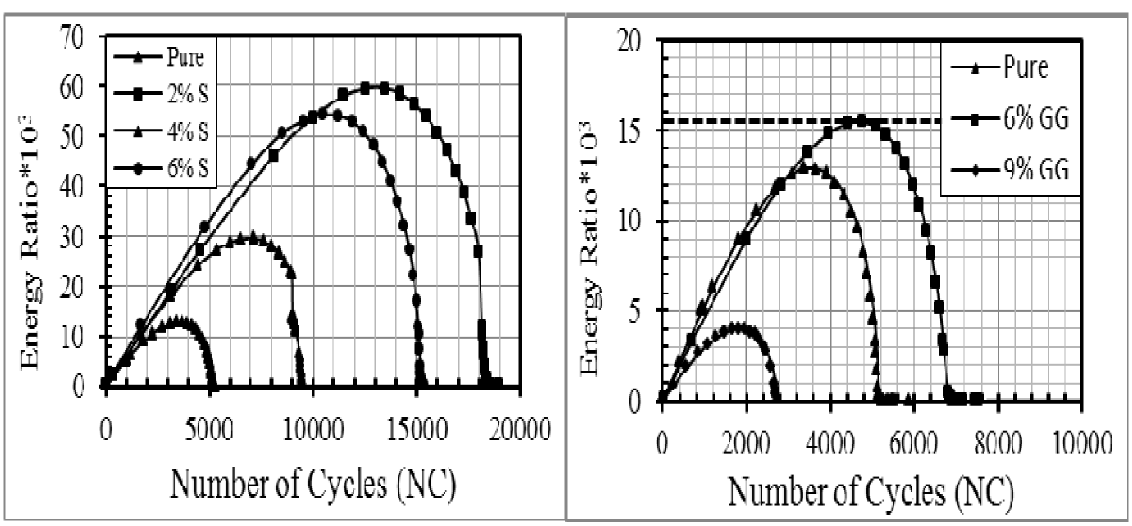

Figure A14. Energy ratio against number of cycles at energy approach.

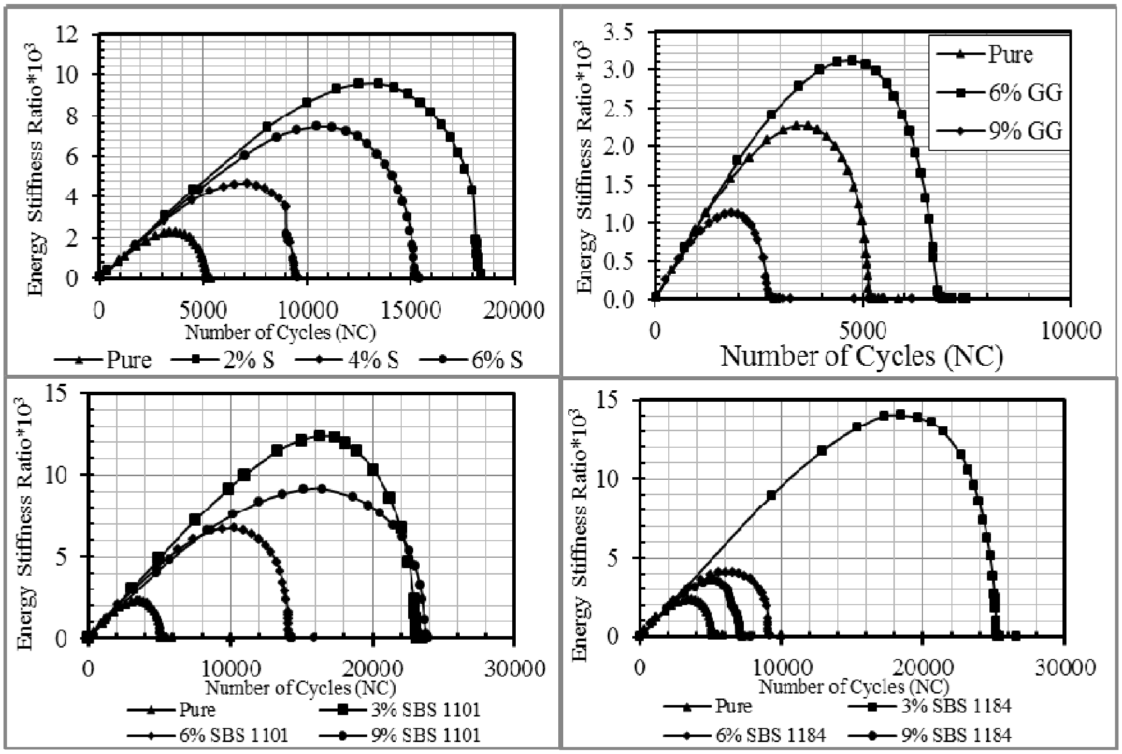

Figure A15. Energy Stiffness Ratio against number of cycles at energy stiffness approach.

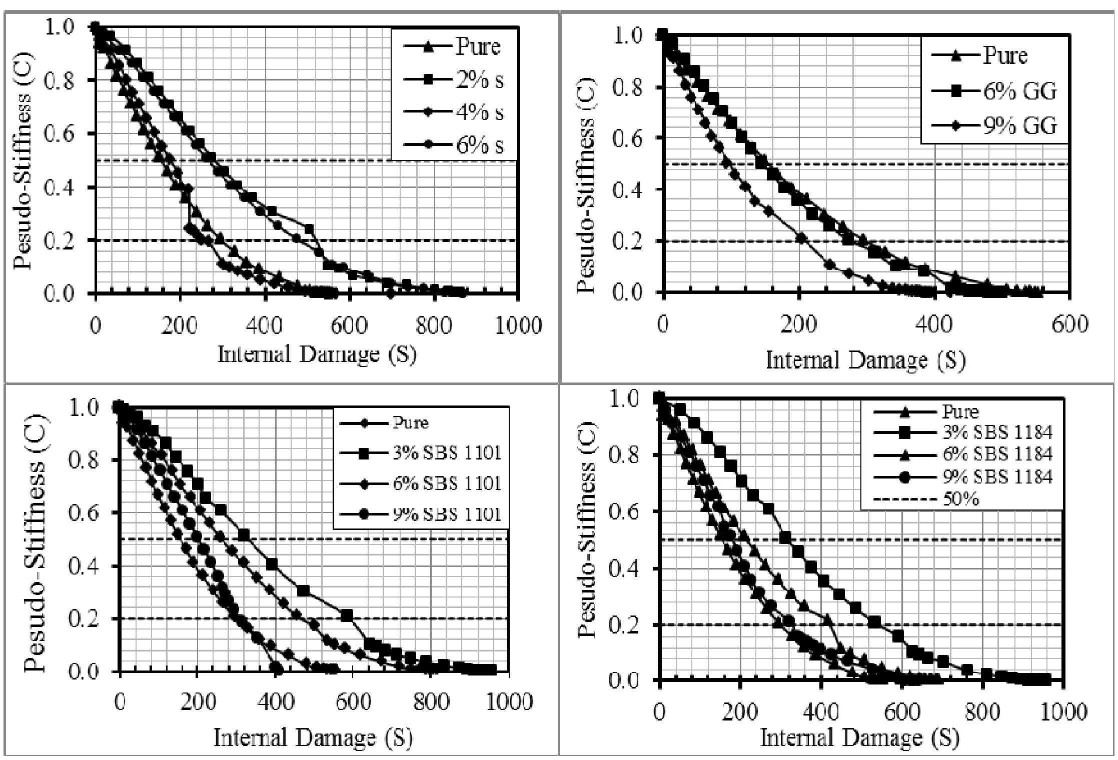

Figure A16. Pseudo-strain-based damage parameter of Durah asphalt binder.


Journal of Civil Engineering and Construction Technology
Related Journals Published by Academic Journals
■ International Journal of Computer Engineering Research
■ Journal of Electrical and Electronics Engineering Research
■ Journal of Engineering and Computer Innovations
■ Journal of Petroleum and Gas Engineering
■ Journal of Engineering and Technology Research
■ Journal of Civil Engineering and Construction Technology
academicJournals